

ARTICLE

# γ-Secretase promotes membrane insertion of the human papillomavirus L2 capsid protein during virus infection

Takamasa Inoue<sup>1</sup>, Pengwei Zhang<sup>2</sup>, Wei Zhang<sup>2</sup>, Kyliia Goodner-Bingham<sup>2</sup>, Allison Dupzyk<sup>1,6</sup>, Daniel DiMaio<sup>2,3,4,5</sup>, and Billy Tsai<sup>1</sup> 

Despite their importance as human pathogens, entry of human papillomaviruses (HPVs) into cells is poorly understood. The transmembrane protease γ-secretase executes a crucial function during the early stages of HPV infection, but the role of γ-secretase in infection and the identity of its critical substrate are unknown. Here we demonstrate that γ-secretase harbors a previously uncharacterized chaperone function, promoting low pH-dependent insertion of the HPV L2 capsid protein into endosomal membranes. Upon membrane insertion, L2 recruits the cytosolic retromer, which enables the L2 viral genome complex to enter the retrograde transport pathway and traffic to the Golgi en route for infection. Although a small fraction of membrane-inserted L2 is also cleaved by γ-secretase, this proteolytic event appears dispensable for HPV infection. Our findings demonstrate that γ-secretase is endowed with an activity that can promote membrane insertion of L2, thereby targeting the virus to the productive infectious pathway.

## Introduction

High-risk human papillomaviruses (HPVs) cause essentially all cancers of the uterine cervix and are also responsible for other anogenital and oropharyngeal cancers (Forman et al., 2012). Although prophylactic vaccines against HPV infection are efficacious (Lee and Garland, 2017), cancers associated with HPV infection remain a major disease burden due to the limited use of the vaccine in some populations and the absence of vaccine benefit in individuals with current HPV infection (Hildesheim et al., 2007). Therefore, determining the cellular basis of HPV entry may reveal new strategies to combat HPV infection.

HPV is a small, nonenveloped DNA tumor virus composed of 72 pentamers of the L1 major capsid protein, with up to 72 copies of the L2 minor capsid protein harbored within the L1-pentameric capsid (Buck et al., 2008). L1 and L2 interact with the ~8-kilobase pair viral DNA genome (Mallon et al., 1987). To enter host cells, L1 binds to heparin sulfate proteoglycans on the plasma membrane or the extracellular matrix (Joyce et al., 1999; Giroglou et al., 2001; Johnson et al., 2009; Cerqueira et al., 2013), triggering conformational changes in the capsid that allow the furin protease to cleave the L2 N terminus (Richards et al., 2006;

Johnson et al., 2009; Cerqueira et al., 2013, 2015; Calton et al., 2017). The virus then binds to an unidentified entry receptor, which promotes endocytosis (Day et al., 2008). The low pH of the early endosome and potentially the action of cyclophilin B trigger partial capsid disassembly, releasing some of the L1 pentamers from the L2-viral genome complex (Smith et al., 2008; Bergant Marušič et al., 2012), which then traffics to the TGN, Golgi apparatus, and ER (Day et al., 2013; Lipovsky et al., 2013; Zhang et al., 2014). Disassembly of the nuclear envelop during mitosis enables the L2-viral genome complex to enter the nucleus (Pyeon et al., 2009; Aydın et al., 2014, 2017; Calton et al., 2017), where transcription and replication of the viral genome occur. Because HPV in the early endosome can also sort to lysosomes for degradation (Bergant Marušič et al., 2012; Schelhaas et al., 2012), proper targeting of the L2-viral genome complex along the Golgi-ER axis likely represents a committed infection step. The molecular details controlling endosome-to-Golgi transport have not been fully established.

Two observations have illuminated this committed step. First, a genome-wide siRNA screen identified the cytosolic retromer

<sup>1</sup>Department of Cell and Developmental Biology, University of Michigan Medical School, Ann Arbor, MI; <sup>2</sup>Department of Genetics, Yale School of Medicine, New Haven, CT; <sup>3</sup>Department of Therapeutic Radiology, Yale School of Medicine, New Haven, CT; <sup>4</sup>Department of Molecular Biophysics and Biochemistry, Yale School of Medicine, New Haven, CT; <sup>5</sup>Yale Cancer Center, New Haven, CT; <sup>6</sup>Department of Microbiology and Immunology, University of Michigan Medical School, Ann Arbor, MI.

Correspondence to Billy Tsai: [btsai@umich.edu](mailto:btsai@umich.edu); Daniel DiMaio: [daniel.dimaio@yale.edu](mailto:daniel.dimaio@yale.edu); W. Zhang's present address is NantCell (Nantworks), Seattle, WA; T. Inoue's present address is Pathogen Research Section, Central Research Laboratory, Research and Development Division, Japan Blood Products Organization, Kobe, Japan.

© 2018 Inoue et al. This article is distributed under the terms of an Attribution-Noncommercial-Share Alike-No Mirror Sites license for the first six months after the publication date (see <http://www.rupress.org/terms/>). After six months it is available under a Creative Commons License (Attribution-Noncommercial-Share Alike 4.0 International license, as described at <https://creativecommons.org/licenses/by-nc-sa/4.0/>).

complex as crucial in targeting HPV from the endosome to the Golgi (Lipovsky et al., 2013). This is consistent with the well-established role of the retromer in transferring cellular transmembrane (TM) protein cargos from endosomal compartments to the TGN (Gallon and Cullen, 2015). Second, the activity of  $\gamma$ -secretase (Beel and Sanders, 2008), a TM protease that cleaves the TM domain of cellular TM protein substrates, is essential during early HPV infection (Huang et al., 2010; Karanam et al., 2010). We found that endosome-to-Golgi trafficking of HPV requires  $\gamma$ -secretase activity (Zhang et al., 2014), but the identity of the crucial  $\gamma$ -secretase substrate remains unknown.

Even though the nonenveloped HPV capsid lacks TM proteins, previous reports suggest that L2 might insert into a host membrane. First, the L2 N terminus contains a conserved, hydrophobic segment that can act as a TM domain (Bronnimann et al., 2013). Second, antibody-staining and protease sensitivity experiments indicate that much of L2 except for the N terminus upstream of this putative TM domain is accessible from the cytoplasmic side of the endosome membrane (DiGiuseppe et al., 2015), indicating that a segment of L2 spans the membrane (Campos, 2017). Third, during entry, L2 binds to the cytosolic retromer, SNX17, and SNX27 proteins (Bergant and Banks, 2013; Pim et al., 2015; Popa et al., 2015), further implying that an L2 segment spans the endosomal membrane to access these cytosolic factors. Finally, an L2 C-terminal segment displays membrane-destabilizing activity (Kämper et al., 2006).

We report here that  $\gamma$ -secretase is endowed with a novel chaperone function, promoting insertion of the HPV L2 protein into endosomal membranes. Insertion in turn enables L2 to recruit the retromer, which targets the virus to the TGN en route for infection. These findings provide important new insight into HPV entry and have implications for the role of  $\gamma$ -secretase in normal cell function and disease.

## Results

### $\gamma$ -Secretase binds to and cleaves the L2 protein of HPV16 and HPV5

HPV pseudoviruses (PsVs) are composed of viral L1 and L2 capsid proteins encapsidating a plasmid encoding a reporter gene, whose expression is used to monitor viral infection. HPV16 PsV has been used to study HPV entry because it largely mimics the behavior of authentic HPV16 and because it allows the construction and analysis of viral mutants (Buck et al., 2004, 2008). To further exploit this system, a 3xFLAG epitope tag was appended to the C terminus of an otherwise WT HPV16 L2 protein (L2-3xFLAG), and an HPV16 PsV containing this L2 protein, designated WT HPV16.L2F, was generated (Zhang et al., 2014). The FLAG tag is constitutively exposed on the surface of the capsid, it does not interfere with particle assembly and cellular entry of HPV, and the tagged L2 protein can be detected in infected cells with an anti-FLAG antibody (Zhang et al., 2014). Infection by WT HPV16.L2F PsV or by HPV16 PsV containing untagged L2 was severely inhibited by  $\gamma$ -secretase inhibition (Zhang et al., 2014).

We used FLAG-tagged HPV16 PsV to identify in an unbiased manner cellular proteins that interact with HPV16 during infection. An extract prepared from HeLa cells infected with WT

HPV16.L2F for 16 h was subjected to immunoprecipitation using anti-FLAG M2 antibody. The precipitated material was eluted from the beads using 3xFLAG peptide, and the eluted sample was analyzed by SDS-PAGE followed by silver staining. As a negative control, an extract of uninfected HeLa cells was incubated with WT HPV16.L2F PsV and then processed as above. We consider proteins that bound to L2 under this control condition to be cellular proteins that associate with the virus during extraction, as opposed to factors that support specific HPV trafficking.

Using this approach, we observed distinct bands that coprecipitated with L2-3xFLAG from the infected cell extract but not from the control extract incubated with PsV (Fig. 1A). The entire eluted samples from both conditions were subjected to shotgun mass spectrometry. The identification of known L2-interacting factors in the infected cell sample, namely, SNX17 and annexin A2 (Bergant Marušič et al., 2012; Woodham et al., 2012), demonstrated that this method can identify proteins that bind incoming virions. Peptides corresponding to all four subunits of the  $\gamma$ -secretase complex (nicastrin [NICA], presenilin-1 [PS1], anterior pharynx-defective 1 [APH1A], and presenilin enhancer 2 [PEN2]) were identified by mass spectrometry from the immunoprecipitates of infected but not control cells (Fig. 1B). The presence of NICA and the C-terminal fragment (CTF) of PS1 in the infected cell immunoprecipitates was confirmed by immunoblotting (Fig. 1C). These findings demonstrate that HPV16 interacts with  $\gamma$ -secretase during infection. XXI, an allosteric inhibitor of  $\gamma$ -secretase that impairs substrate binding to  $\gamma$ -secretase (Li et al., 2014), blocked the interaction between L2 and PS1 (Fig. 1D, top, lane 3), suggesting that L2 is a  $\gamma$ -secretase substrate.

We also analyzed HPV5 PsV, a cutaneous HPV type associated with skin cancer, which is also blocked by  $\gamma$ -secretase inhibition (Wang and Roden, 2013; Kwak et al., 2014). The anti-FLAG antibody coimmunoprecipitated PS1 CTF from extracts of cells infected with HPV5 PsV containing 3xFLAG-tagged L2 (WT HPV5.L2F) but not from extracts of uninfected cells incubated with HPV5 PsV (Fig. 1E). These results demonstrate that  $\gamma$ -secretase also binds to HPV5, indicating that this enzyme interacts with both mucosal and cutaneous HPV genotypes.

Binding of  $\gamma$ -secretase to HPV during entry raised the possibility that L2 is cleaved by  $\gamma$ -secretase. To test this, HeLa cells transfected with either control scrambled (Scr) siRNA or with two different siRNAs each against  $\gamma$ -secretase subunits PS1 or PEN2 were infected with WT HPV16.L2F for 16 h. Infected cell extracts were subjected to SDS-PAGE followed by immunoblotting using an anti-FLAG antibody. In the extract of cells transfected with control siRNA, we observed bands corresponding to full-length L2-3xFLAG and smaller L2 species that likely represent cleaved forms of L2, which we designated L2-3xFLAG\* (Fig. 1F, top, lane 1), although most L2 proteins were not cleaved. Because the FLAG tag is present at the C terminus of L2, detection of L2-3xFLAG\* with an anti-FLAG antibody implied that cleavage occurred near the N terminus of L2. Depleting PS1 or PEN2 with any of the siRNAs blocked the generation of L2-3xFLAG\* (Fig. 1F, top, lanes 2–5). These findings demonstrate that  $\gamma$ -secretase is required for the appearance of the cleaved forms of L2. Knockdown of PS1 and PEN2 was confirmed by immunoblotting (Fig. 1F). Knocking down PS1 also down-regulated PEN2 expression, while silencing

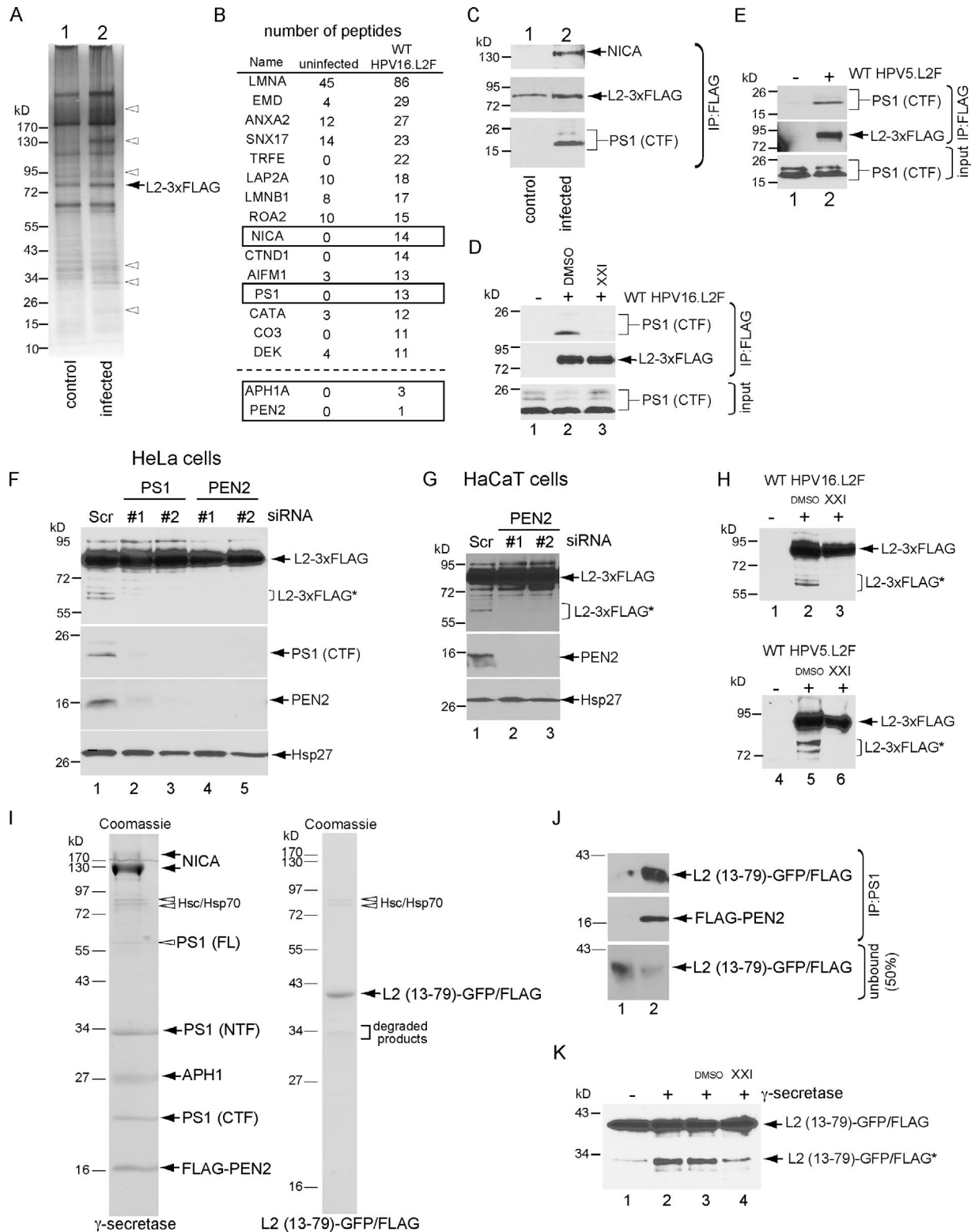


Figure 1.  $\gamma$ -Secretase binds to and cleaves the L2 protein of HPV16 and HPV5. (A) HeLa cells were infected with WT HPV16.L2F at MOI = 100 for 16 h. The resulting whole-cell lysate (WCL) was subjected to immunoprecipitation using anti-FLAG M2 antibody, and the bound proteins were eluted with 3xFLAG peptide. As a control, a WCL from uninfected cells was mixed with WT HPV16.L2F and subjected to the same immunoprecipitation procedure. Both samples were resolved by SDS-PAGE followed by silver staining. The open arrowheads indicate bands present only in the immunoprecipitate from infected cells. (B) Immunoprecipitated samples prepared in A were subjected to shotgun mass spectrometry. Proteins represented by >10 peptides from the WT HPV16.L2F-infected samples are listed, including  $\gamma$ -secretase subunits NICA and PS1, as are two subunits of the  $\gamma$ -secretase complex with <10 peptides identified, APH1A and PEN2. ANXA2, annexin A2. (C) Immunoprecipitated samples from A were analyzed by immunoblotting with antibodies recognizing NICA, FLAG, or PS1 CTF. (D) HeLa cells were uninfected or infected with WT HPV16.L2F for 16 h in the presence of DMSO or  $\gamma$ -secretase inhibitor XXI (1  $\mu$ M). WCLs were electrophoresed directly (input) or subjected to immunoprecipitation using anti-FLAG M2 antibody, and the bound proteins were eluted with SDS-sample buffer

PEN2 decreased the abundance of the PS1 CTF, consistent with a previous report (Takasugi et al., 2003). PEN2-dependent cleavage of HPV16 L2 was also observed in immortalized human HaCaT keratinocytes (Fig. 1 G, top). Thus,  $\gamma$ -secretase-dependent cleavage of L2 occurs in two epithelial cell types susceptible to HPV infection. We also tested the effect of the chemical  $\gamma$ -secretase inhibitor XXI on L2 cleavage. Fig. 1 H shows that addition of 1  $\mu$ M XXI at the time of infection inhibited cleavage of HPV16 and HPV5 L2-3xFLAG in infected HeLa cells. These data strongly suggest that  $\gamma$ -secretase cleaves L2 in infected cells.

To establish that  $\gamma$ -secretase binds to and cleaves L2 directly, we reconstituted the binding and cleavage reactions using purified components. We isolated enzymatically active  $\gamma$ -secretase from 293T cells transfected with genes encoding the  $\gamma$ -secretase subunits (Lu et al., 2014). The purified  $\gamma$ -secretase complex contained NICA, APH1, PEN2, and the N-terminal fragment and CTF of PS1, as well as trace amounts of full-length PS1 and the Hsc/Hsp70 chaperones (Fig. 1 I, left). Autocleavage of full-length PS1 generates PS1 N-terminal fragment and CTF, indicating that  $\gamma$ -secretase assembled in the transfected 293T cells or in vitro is likely enzymatically active. We also purified a fusion protein consisting of N-terminal HPV16 L2 residues 13–79 fused in frame to GFP and FLAG (L2 [13–79]–GFP/FLAG; Fig. 1 I, right). This L2 segment, which contains the putative TM domain (aa 45–67), corresponds to the N terminus of L2 following cleavage by furin. The L2 (13–79)–GFP/FLAG preparation contained a small amount of truncated protein. When purified L2 (13–79)–GFP/FLAG was incubated with or without purified  $\gamma$ -secretase in the presence of the detergent CHAPSO, L2 (13–79)–GFP/FLAG coimmunoprecipitated with the  $\gamma$ -secretase (Fig. 1 J). Moreover, when these two purified proteins were incubated together, an ~34-kD cleaved form designated L2 (13–79)–GFP/FLAG\* was generated (Fig. 1 K); similar to the situation in infected cells, only a small fraction of L2 (13–79)–GFP/FLAG was cleaved. As expected, generation of L2 (13–79)–GFP/FLAG\* in vitro was inhibited by XXI (Fig. 1 K, lane 4). These findings demonstrate that  $\gamma$ -secretase binds directly to L2, enabling the protease to cleave aa 13–79 of L2, which contains the putative TM domain near the L2 N terminus.

#### $\gamma$ -Secretase engages and cleaves L2 in the endosome after furin-mediated cleavage

Cleavage of L2 by furin at the cell surface is thought to be one of the earliest steps during HPV entry (Richards et al., 2006; Johnson et al., 2009; Wang and Roden, 2013). Therefore, it was likely that  $\gamma$ -secretase binding to and cleavage of L2 occurs after furin cleavage. We tested the effect of the furin inhibitor dRVKR on the interaction between L2 and  $\gamma$ -secretase in infected cells.

As shown in Fig. S1, dRVKR inhibited binding of L2 to  $\gamma$ -secretase (Fig. S1 A, lane 3) and cleavage of L2 (Fig. S1 B, lane 3). These findings indicate that cleavage of L2 by  $\gamma$ -secretase requires prior furin-mediated cleavage. Moreover, whereas HPV16.L2F infection (as assessed by expression of the luciferase reporter gene) was reduced by 50% if XXI was added at 6 h post-infection (hpi; Fig. S1 C, solid line), dRVKR caused half-maximal inhibition of HPV16 infection at 2 hpi (Fig. S1 C, dotted line), suggesting that  $\gamma$ -secretase acts after furin during HPV entry.

To determine when  $\gamma$ -secretase engages and cleaves L2, we performed time course experiments. HeLa cells were infected with WT HPV16.L2F and harvested at various time points from 0 to 16 hpi. The resulting cell extracts were subjected to immunoprecipitation using an anti-FLAG antibody and immunoblotted with anti-PS1 antibody to assess formation of a complex between the capsid and  $\gamma$ -secretase and with anti-FLAG antibody to assess L2 cleavage. PS1 bound L2 beginning at 6 hpi (Fig. S1 D, top), with L2 cleavage being evident by 8 hpi (Fig. S1 D, middle). Consistent with this observation, XXI started to lose its ability to block L2 cleavage when it was added at 6 or more hpi (Fig. S1 E). Because HPV reaches the endosome by 6–8 hpi and the Golgi by 16 hpi (Popa et al., 2015), these findings imply that  $\gamma$ -secretase interacts with and cleaves L2 in the endosome.

#### The L2 protein is inserted into a host cell membrane during entry

To be cleaved by  $\gamma$ -secretase, L2 must first insert into a cell membrane because all known  $\gamma$ -secretase substrates are TM proteins (Beel and Sanders, 2008). Although previous studies suggested that L2 may adopt a TM topology during entry (Bronnimann et al., 2013; DiGiuseppe et al., 2015; Campos, 2017) direct biochemical evidence of L2 in this configuration is lacking. To determine whether there is a membrane-inserted form of L2 during infection, we used the classic alkali extraction approach, a rigorous biochemical method that assesses if a protein is an integral TM protein (Fujiki et al., 1982). HeLa cells infected with WT HPV16.L2F for 16 h were mechanically homogenized, and the membrane fraction (including plasma, endosome, Golgi, and ER membranes) was isolated by centrifugation. This fraction was treated with nuclease in the presence of the reducing reagent DTT, and then resuspended in an alkaline carbonate solution containing the denaturant urea and subjected to further centrifugation to generate a supernatant (S) and a pellet (P) fraction. Because alkali treatment disrupts the integrity of membranes without compromising the ability of a TM protein to remain as a membrane-integrated protein, soluble luminal proteins (such as protein disulfide isomerase [PDI]) and peripherally associated

and analyzed by SDS-PAGE and immunoblotting with antibodies recognizing FLAG and PS1 (CTF). (E) As in D, except HeLa cells were uninfected or infected with WT HPV5.L2F for 16 h. (F) HeLa cells transfected with the indicated siRNAs were infected with WT HPV16.L2F. WCLs were analyzed by immunoblotting with antibodies recognizing FLAG, PS1 (CTF), PEN2, and Hsp27 as a loading control. The L2-3xFLAG\* putative  $\gamma$ -secretase cleavage product is indicated. (G) As in F, except HaCaT cells were used. (H) HeLa cells were uninfected or infected with WT HPV16.L2F (lanes 1–3) or WT HPV5.L2F (lanes 4–6) for 16 h in the presence of 0.1% DMSO or 1  $\mu$ M XXI. The resulting WCLs were analyzed by SDS-PAGE and immunoblotting with an anti-FLAG antibody. (I) Coomassie staining of purified recombinant  $\gamma$ -secretase complex (left) and L2 (13–79)–GFP/FLAG (right). (J) HPV16 L2 (13–79)–GFP/FLAG was incubated with or without recombinant  $\gamma$ -secretase complex for 16 h. The  $\gamma$ -secretase complex was precipitated using a PS1 antibody, and the precipitated material was analyzed by SDS-PAGE and immunoblotted with the indicated antibodies. (K) HPV16 L2 (13–79)–GFP/FLAG was incubated with or without recombinant  $\gamma$ -secretase complex for 16 h. Where indicated, DMSO or XXI was added. Samples were then analyzed by SDS-PAGE and immunoblotted with an anti-GFP antibody.

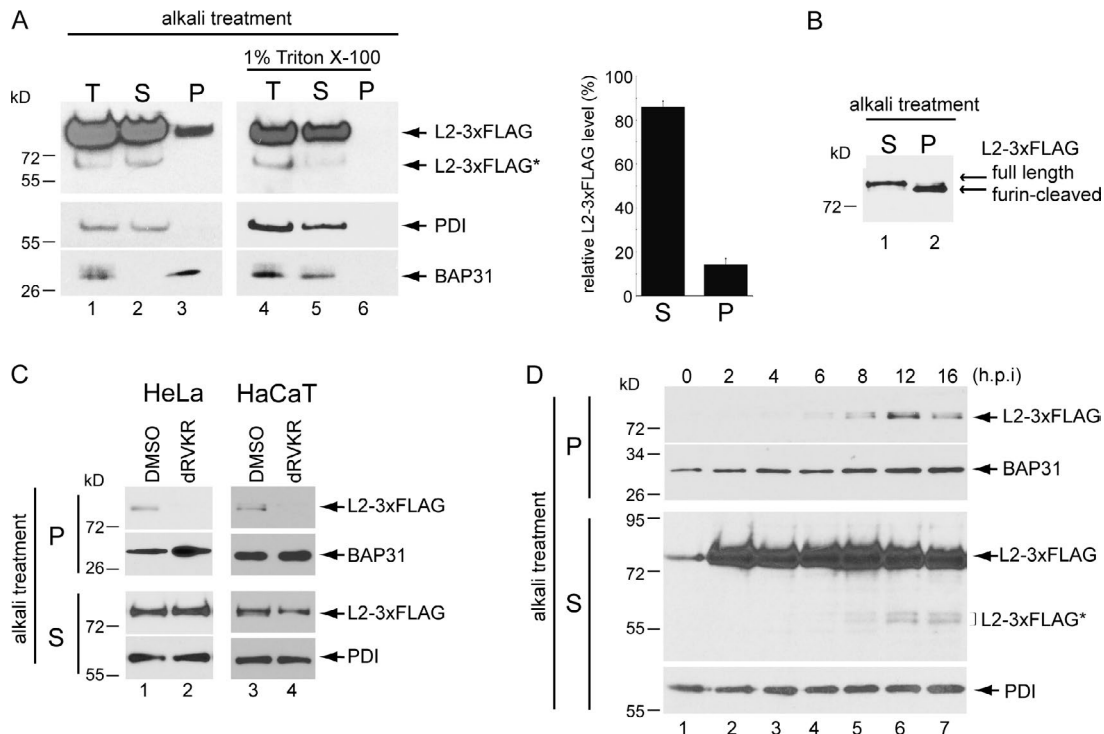


**Figure 2. The HPV16 L2 protein inserts into host cell membranes.** (A) HeLa cells infected with WT HPV16.L2F at MOI = 50 for 16 h were homogenized, and the membrane fraction was separated from the nuclear, mitochondrial, and cytosol fractions. The total membrane fraction (T) was incubated in 0.1 M sodium carbonate (pH 11.3; alkali treatment) supplemented with urea and DTT in the absence or presence of 1% Triton X-100 and centrifuged at 100,000 g for 10 min. The resulting S and P fractions were analyzed by SDS-PAGE and immunoblotting with antibodies recognizing FLAG, PDI, and BAP31. PDI and BAP31 serve as marker proteins for ER luminal and membrane proteins, respectively. Graph depicts the relative levels of L2-3xFLAG in the S and P fractions. Data represents the means  $\pm$  standard deviations of data from at least three independent experiments. (B) Equal amounts of L2-3xFLAG in the S and P fractions in A in the absence of triton X-100 were subjected to SDS-PAGE, followed by immunoblotting with anti-FLAG antibody. (C) HeLa (lanes 1 and 2) and HaCaT (lanes 3 and 4) cells infected with WT HPV16.L2F at MOI = 50 were treated with 0.1% DMSO or 1  $\mu$ M dRVKR. At 8 hpi, membrane fractions were subjected to alkali treatment as in A in the absence of Triton X-100. The resulting P and S fractions were analyzed by SDS-PAGE and immunoblotting with antibodies recognizing FLAG and PS1 (CTF). (D) Infection was initiated by adding WT HPV16.L2F to the medium of HeLa cells at 0 hpi at MOI = 50. At the indicated time points, cells were harvested, and the resulting membrane fractions were subjected to alkali treatment in the absence of Triton X-100, followed by centrifugation as in A. The resulting S and P fractions were analyzed by SDS-PAGE and immunoblotting with the indicated antibodies.

membrane proteins are released into the S fraction, while TM proteins (such as BAP31) remain in the P fraction (Fig. 2 A, middle and bottom, lanes 1–3). Urea and DTT were included during sample preparation to disrupt the virus particle so that only membrane-integrated L2 remains in the P fraction.

Using this method, we found that a small amount of L2-3xFLAG was present in the P fraction corresponding to membrane-inserted L2 (Fig. 2 A, top, lane 3; quantified in the graph). The presence of L2 in this fraction was not due to aggregation because, like the TM protein standard BAP31, it was extracted by Triton X-100, a detergent that disrupts membranes (Fig. 2 A, lane 6). The  $\gamma$ -secretase-cleaved form of L2 was not detected in the P fraction, but this might reflect the sensitivity of the experiment. No L1 protein was detected in the P fraction (data not shown). When comparable amounts of soluble and pelleted L2 were analyzed, L2-3xFLAG in the P fraction was observed to migrate slightly faster than L2-3xFLAG in the S fraction (Fig. 2 B), showing that a short form of L2-3xFLAG preferentially inserted into the membrane. Inhibiting furin activity by dRVKR blocked the appearance of L2-3xFLAG in the P fraction in both HeLa and HaCaT cells (Fig. 2 C, top). These data suggest that furin-dependent cleavage of L2 is required for membrane inser-

tion and that the furin-cleaved form of L2 preferentially inserts into the membrane.

We also performed a time course experiment to examine when L2 inserts into the membrane. L2-3xFLAG was first detected in the P fraction at  $\sim$ 6 hpi (Fig. 2 D, top), similar to the time when L2 binding and cleavage by  $\gamma$ -secretase were first detected. This timing suggests that L2 is inserted into the early endosome membrane.

#### **$\gamma$ -Secretase acts as a chaperone to drive low pH-dependent membrane insertion of the L2 protein**

To test whether  $\gamma$ -secretase was required for membrane insertion of L2, we used siRNAs to deplete PS1 or PEN2 from HeLa cells infected with WT HPV16.L2F. Strikingly,  $\gamma$ -secretase depletion blocked insertion of L2-3xFLAG into the membrane without affecting insertion of the control TM protein, BAP31 (Fig. 3 A, top two panels). The  $\gamma$ -secretase inhibitor XXI also inhibited membrane insertion (Fig. 3 B, top, lane 3). Collectively, these results demonstrate that the  $\gamma$ -secretase is essential for membrane insertion of L2. Thus, in addition to its well-characterized protease activity (Beel and Sanders, 2008),  $\gamma$ -secretase is also endowed with a novel nonproteolytic chaperone activity that promotes membrane integration of a soluble protein substrate.

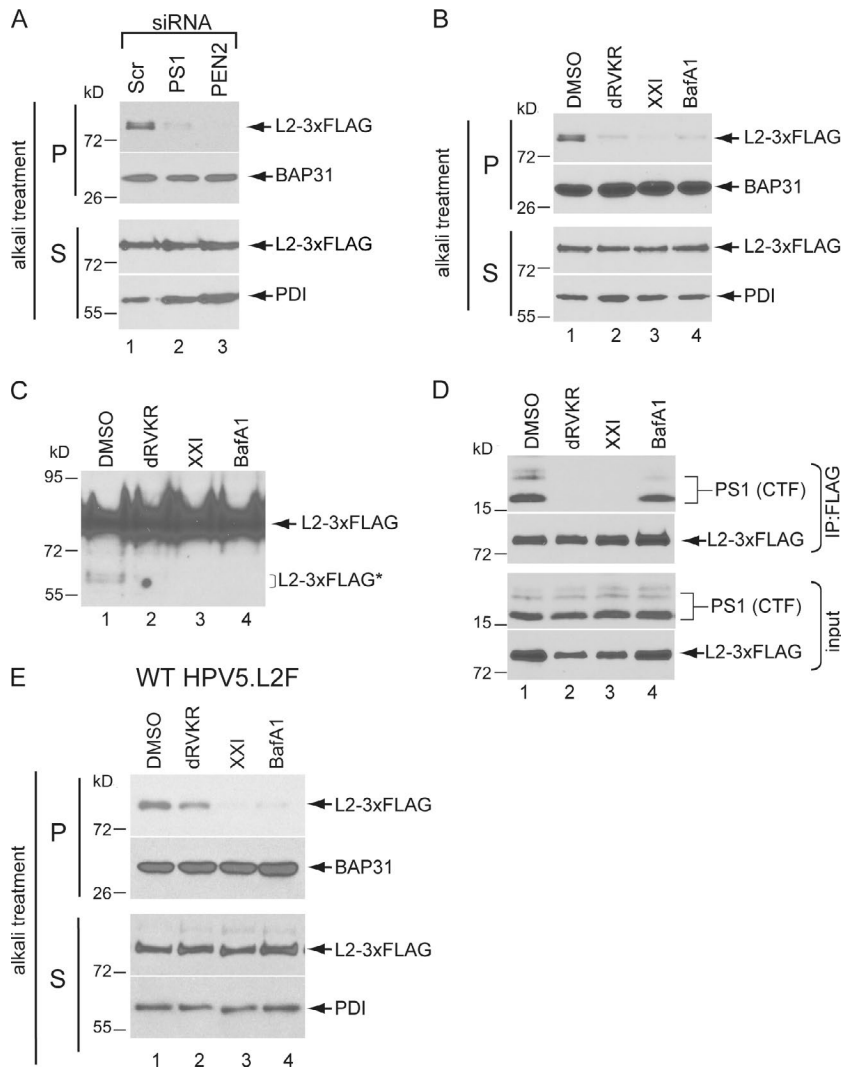


**Figure 3.  $\gamma$ -Secretase drives low pH-dependent membrane insertion of the L2 protein.** (A) HeLa cells transfected with either Scr, PS1, or PEN2 siRNA were infected with WT HPV16.L2F at MOI = 50. Cells were harvested at 8 hpi and processed as in Fig. 4 A in the absence of Triton X-100. The resulting S and P fractions were analyzed by SDS-PAGE and immunoblotting with antibodies recognizing FLAG, PDI, and BAP31. (B) As in A, except that HeLa cells were treated with 0.1% DMSO, 1  $\mu$ M dRVKR, 1  $\mu$ M XXI, or 30 nM BafA1 at the time of infection. (C) The S fractions in B were subjected to SDS-PAGE, followed by immunoblotting with an antibody recognizing FLAG. (D) HeLa cells were infected with WT HPV16.L2F at MOI = 50 in the presence of 0.1% DMSO, 1  $\mu$ M dRVKR, 1  $\mu$ M XXI, or 30 nM BafA1. Cells were harvested at 8 hpi and subjected to immunoprecipitation with anti-FLAG antibody, followed by SDS-PAGE and immunoblotting with antibodies recognizing PS1 (CTF) and FLAG. (E) Same as B, except WT HPV5.L2F was used.

Because membrane insertion of L2 appears to take place in the endosome, we asked if perturbing endosomal acidification with Bafilomycin A1 (BafA1) affected the integration of L2 into the membrane. BafA1 treatment blocks HPV16 infection (Schelhaas et al., 2012). Fig. 3 B shows that BafA1, like dRVKR and XXI, inhibited L2 membrane insertion (Fig. 3 B, top, lane 4) and cleavage (Fig. 3 C, lane 4). Notably, however, BafA1 treatment did not impair interaction of L2 with  $\gamma$ -secretase (Fig. 3 D, top, lane 4), in contrast to dRVKR or XXI. These data suggest that interaction between  $\gamma$ -secretase and L2 is not sufficient for  $\gamma$ -secretase-mediated membrane insertion and cleavage of L2. Rather, another distinct event—a low-pH trigger—acts in concert with  $\gamma$ -secretase to drive insertion of L2 into the endosome membrane so cleavage can occur.

Using the same assay, we showed that the HPV5 L2 protein is also inserted into the membrane (Fig. 3 E, top, lane 1). Membrane insertion of HPV5 L2 was blocked by XXI and BafA1 (Fig. 3 E, top, lanes 3 and 4), but it was only modestly reduced by dRVKR (Fig. 3 E, top, lane 2), consistent with a previous report that HPV5 infection is moderately impaired by furin inhibition (Kwak et al., 2014). These results demonstrate that  $\gamma$ -secretase promotes low pH-dependent membrane insertion of L2 of at least two different HPV types.

### $\gamma$ -Secretase-dependent membrane insertion but not cleavage of L2 promotes HPV infection

Our findings demonstrate that  $\gamma$ -secretase promotes both membrane insertion and cleavage of L2. Whether either or both of these activities are required to support HPV infection is unclear. To test this, we used the CRISPR/Cas9 system to generate two distinct HeLa cell strains in which the PS1 subunit of  $\gamma$ -secretase is knocked out (HeLa PS1 CRISPR knockout [KO] #1 and #2; Fig. S2 A). The sequence of the mutations is shown in Fig. S2 B. Consistent with transient knockdown of PS1 by siRNA, when either PS1 KO cells were infected with WT HPV16.L2F, cleavage of L2 and infection were severely blocked (Fig. 4 A, lane 1; and Fig. S2, C and D).

Add-back of WT PS1 in either strain of PS1 KO cells supported cleavage of L2 (Fig. 4 A and Fig. S3 A, top, compare lane 2 with lane 1); as expected, treatment with XXI blocked L2 cleavage induced by WT PS1 (Fig. 4 A and Fig. S3 A, top, compare lane 3 with lane 2). However, when either of two previously characterized PS1 mutants that cannot cleave the cellular substrate amyloid precursor protein (L166P and F237I; Sun et al., 2017) were added back to either of the PS1 KO cell strains, cleavage of L2 was negligible (Fig. 4 A and Fig. S3 A, lanes 4 and 5). We conclude that in

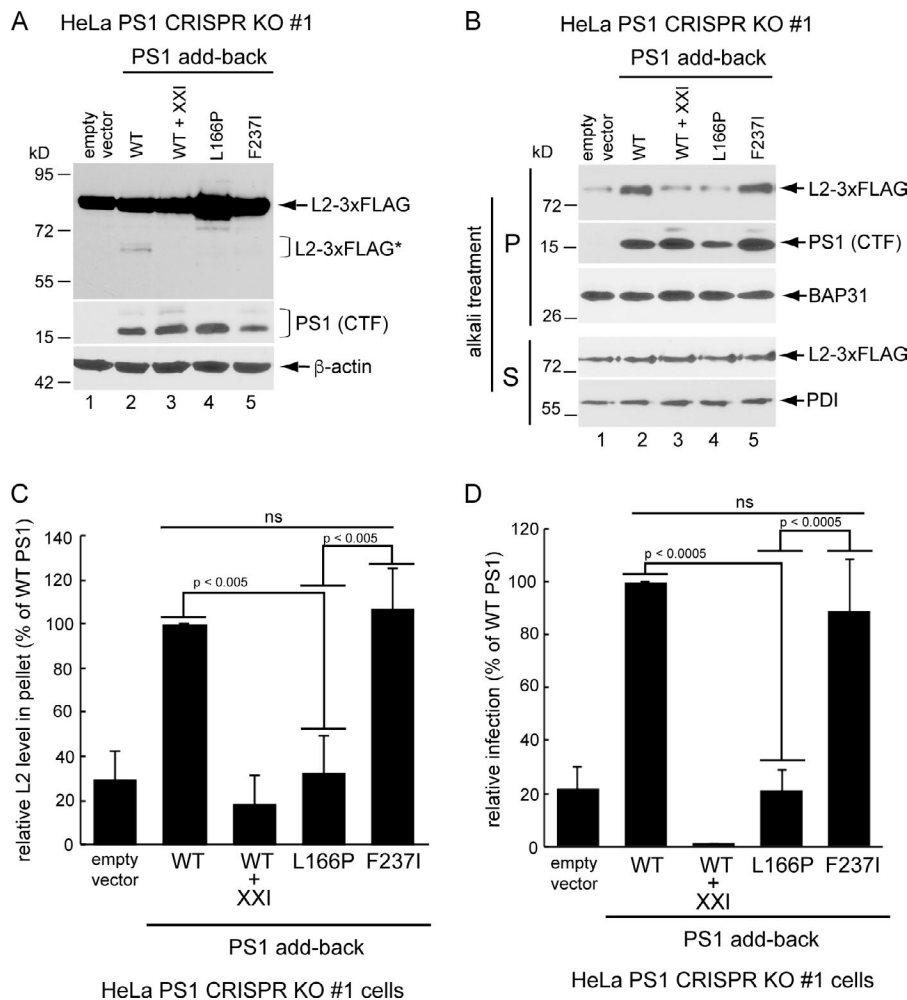


**Figure 4.  $\gamma$ -Secretase-dependent membrane insertion of L2 but not L2 cleavage promotes HPV infection.** (A) HeLa PS1 CRISPR KO #1 cells transfected with the indicated constructs were infected with WT HPV16.L2F at MOI = 100 for 16 h in the absence or presence of 1  $\mu$ M XXI. The resulting WCLs were subjected to anti-FLAG immunoprecipitation, followed by SDS-PAGE and immunoblotting with antibodies recognizing FLAG, PS1 (CTF), and  $\beta$ -actin as a loading control. (B) HeLa PS1 CRISPR KO #1 cells transfected with the indicated constructs were infected with WT HPV16.L2F at MOI = 50 for 12 h in the absence or presence of 1  $\mu$ M XXI. Cells were harvested and processed as in Fig. 4 A in the absence of Triton X-100. The resulting S and P fractions were analyzed by SDS-PAGE and immunoblotting with antibodies recognizing FLAG, PS1, PDI, and BAP31. (C) The intensity of the full-length L2 band in the P fraction in B was quantified with ImageJ (National Institutes of Health). Data are normalized to values for PS1 KO cells expressing WT PS1 and represent the means  $\pm$  standard deviations of data from at least three independent experiments. Student's two-tailed t test was used to assess statistical significance. (D) HeLa PS1 CRISPR KO #1 cells transfected with the indicated constructs were infected at MOI = 100 with WT HPV16.L2F containing a reporter plasmid expressing secreted luciferase. At 36 hpi, luciferase activity was measured in culture supernatant. Luciferase activity is normalized to the value derived from WT PS1-transfected cells, which is set at 100%. All infection values represent the means  $\pm$  standard deviations of data from at least three independent experiments. Student's two-tailed t test was used to assess statistical significance.

contrast to WT PS1, L166P and F237I PS1 poorly support cleavage of L2. The mutants are expressed at comparable levels as WT PS1 (Fig. 4 A, bottom).

When these PS1 mutants were examined for their ability to promote membrane insertion of L2 using the same add-back strategy, we found that F237I but not L166P PS1 supported membrane insertion of L2 to the same extent as WT PS1 (Fig. 4 B and Fig. S3 B, top, compare lanes 5 and 4 with lane 2; the extent of L2 membrane insertion is quantified in Fig. 4 C and Fig. S3 C). Hence, F237I PS1 fully supports membrane insertion of L2, although it cleaves this viral protein inefficiently. In contrast, the L166P PS1 mutant poorly supports both membrane insertion and cleavage.

Strikingly, we found that add-back of F237I PS1 largely restores HPV infection when compared with WT PS1 (Fig. 4 D and Fig. S3 D, compare fifth bar with second bar). Because F237I PS1 promotes HPV infection efficiently despite the fact that it cleaves L2 poorly, these data strongly argue that  $\gamma$ -secretase-induced cleavage of L2 is dispensable for HPV infection. Add-back of L166P PS1 does not restore HPV infection when compared with WT PS1 (Fig. 4 D and Fig. S3 D, compare fourth bar with second bar). Since L166P PS1 does not promote membrane insertion (or cleavage) of L2, these findings also indicate that membrane insertion of L2 by  $\gamma$ -secretase is required to promote HPV infection.

### A TM L2 GxxxG motif is required for binding to $\gamma$ -secretase and targeting HPV to the Golgi during infection

GxxxG motifs are frequently found in TM domains and mediate TM helix-helix interactions in a variety of systems (Russ and Engelman, 2000). There are three highly conserved GxxxG motifs (<sup>52</sup>GxxxG<sup>56</sup>, <sup>57</sup>GxxxG<sup>61</sup>, and <sup>59</sup>GxxxG<sup>63</sup>) located within the N-terminal putative TM domain of HPV16 L2 (Bronnimann et al., 2013). HPV16 PsV harboring an L2 mutant in which a conserved glycine at position 57 or 61 is mutated to valine cannot efficiently infect cells, even though when expressed in a heterologous system, it is inserted into the bacterial cell membrane (Bronnimann et al., 2013). To test the importance of the L2 TM GxxxG motifs in engaging  $\gamma$ -secretase during HPV entry, glycines at positions 57 and 61 were simultaneously mutated to valine, and an HPV16 PsV containing 3xFLAG-tagged L2 with these mutations (designated GV HPV16.L2F) was produced. As expected, GV HPV16.L2F was severely defective for infection in HeLa and HaCaT cells (Fig. 5 A). In cells infected with GV HPV16.L2F, the mutant L2 protein failed to bind to  $\gamma$ -secretase (Fig. 5 B, top, lane 2), did not insert into the membrane (Fig. 5 C, lane 2), and was not cleaved by  $\gamma$ -secretase (Fig. 5 D, lane 2). These findings imply that the L2 GV mutant harbors structural changes that preclude it from properly engaging  $\gamma$ -secretase during infection. This would pre-

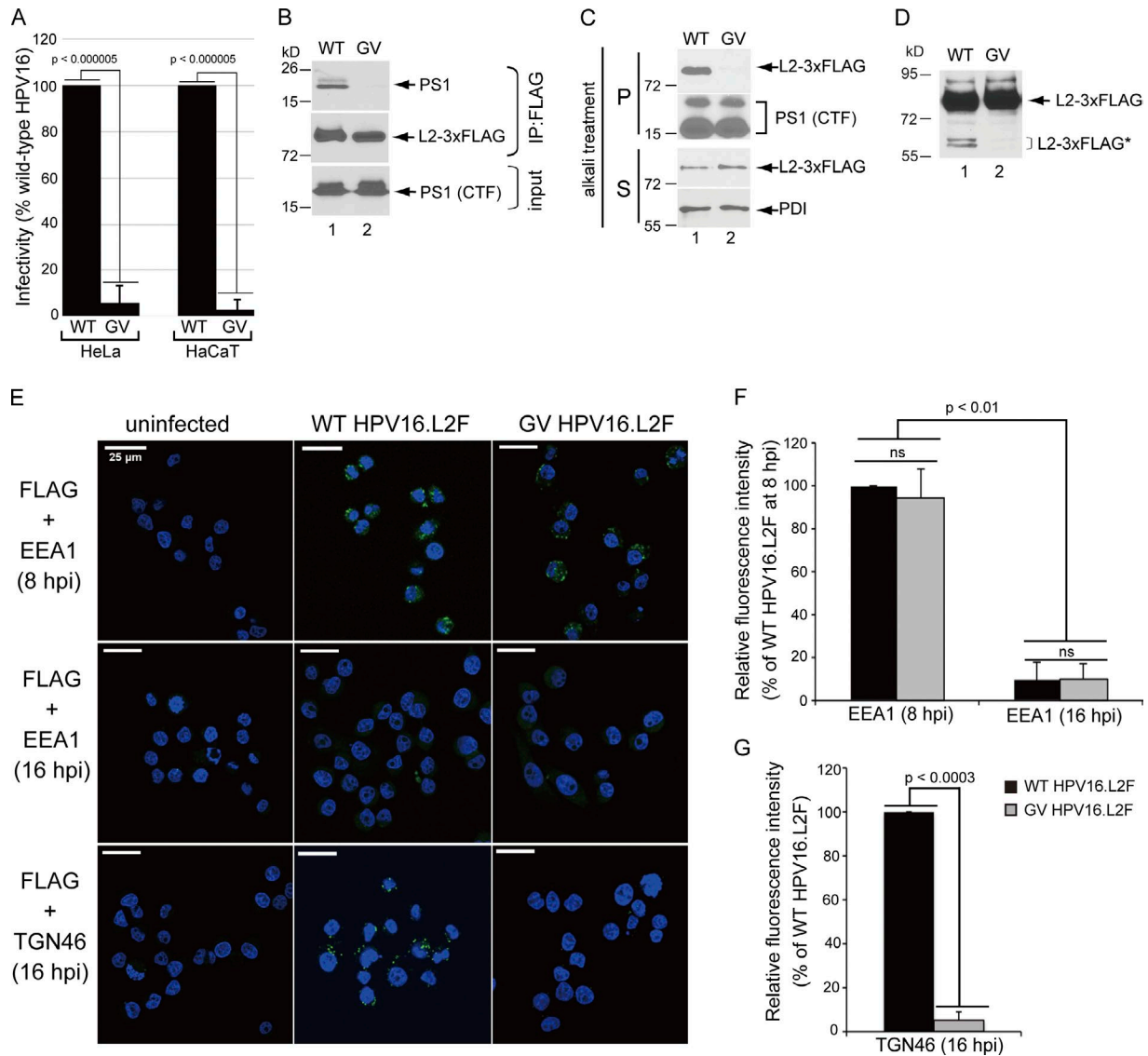


**Figure 5. An L2 GxxxG motif is required for binding to  $\gamma$ -secretase that targets HPV to the Golgi during infection.** (A) HeLa or HaCaT cells were infected with WT or GV HPV16.L2F containing an equal number of packaged reporter plasmids expressing HcRed. At 48 hpi, cells were analyzed by flow cytometry for HcRed expression. Fraction of HcRed-expressing cells is shown relative to cells infected with WT HPV16.L2F, which is set at 100%, and represents the means  $\pm$  standard deviations of data from at least three independent experiments. Student's two-tailed *t* test was used to assess statistical significance. (B) HeLa cells were infected at MOI = 100 with WT HPV16.L2F or with GV HPV16.L2F containing an equivalent number of packaged genomes for 16 h and lysed. The resulting WCLs were subjected to immunoprecipitation with an anti-FLAG antibody. Immunoprecipitated samples were analyzed by SDS-PAGE and immunoblotting with antibodies recognizing PS1 (CTF) or FLAG. (C) HeLa cells infected with WT or GV HPV16.L2F as in B were harvested at 8 hpi and processed as in Fig. 4 A in the absence of Triton X-100. The resulting S and P fractions were analyzed by immunoblotting with antibodies recognizing FLAG, PS1 (CTF), and PDI. PS1 (CTF) and PDI serve as marker proteins for membrane and luminal proteins, respectively. (D) HeLa cells were infected with WT or GV HPV16.L2F. Cells were harvested at 16 hpi and lysed, and the resulting WCLs were analyzed by SDS-PAGE and immunoblotting with an antibody recognizing FLAG. (E) HeLa cells were uninfected or infected with WT or GV HPV16.L2F for 8 or 16 h and subjected to the PLA assay using antibodies recognizing FLAG and either EEA1 or TGN46, as indicated. PLA signals are shown in green. Nuclei were stained with DAPI (blue). (F) Images from WT or GV HPV16.L2F-infected cells for EEA1 PLA at 8 and 16 hpi in E were processed by Blobfinder software to determine the PLA fluorescence intensity per cell in each sample. The average EEA1/L2-3xFLAG intensity was normalized to the control sample infected with WT HPV16.L2F at 8 hpi and represents the means  $\pm$  standard deviations of data from at least three independent experiments. Student's two-tailed *t* test was used to assess statistical significance. Black bars, WT HPV16.L2F; gray bars, GV HPV16.L2F. (G) As in F, except images from WT HPV16.L2F- or GV HPV16.L2F-infected cells for TGN46 PLA in E were processed, and the normalized average TGN46/L2-3xFLAG intensities are shown.

vent it from being inserted into the membrane, which is essential for infection.

To test whether GV HPV16.L2F can enter cells and reach specific intracellular compartments, we used a proximity ligation assay (PLA), which is an immune-based assay that produces a fluorescent signal when two target proteins are localized within

40 nm of each other. When one of the proteins is a marker for a cellular compartment, PLA provides a sensitive assay for the presence of the other protein in or near that compartment. HeLa cells were infected with WT HPV16.L2F or GV HPV16.L2F, fixed, incubated with antibodies recognizing FLAG (which recognized the tagged L2 protein) and early endosome antigen 1 (EEA1; an

endosome marker), and subjected to PLA to detect localization of HPV in the endosome. No PLA signal was generated in mock infected cells (Fig. 5 E). However, in cells infected with either WT HPV16.L2F or GV HPV16.L2F, bright FLAG-EEA1 PLA signals were observed at 8 hpi (Fig. 5 E, top; quantified in Fig. 5 F). These results indicate that the GV virus can enter host cells and reach the endosome. At 16 hpi, the level of endosome-localized virus markedly decreased for both the WT and mutant virus (Fig. 5 E, middle; quantified in Fig. 5 F), presumably because the virus has sorted out of this compartment.

To determine if the mutant L2 protein arrived at the Golgi, we conducted PLA with antibodies recognizing FLAG and TGN46 (a trans-Golgi marker). Whereas WT L2 was detected in the TGN at 16 hpi, only a very low level of the GV mutant was detected in the TGN (Fig. 5 E, bottom; quantified in Fig. 5 G). These results demonstrate that WT but not GV mutant L2 traffics to the TGN after exiting the endosome, suggesting that the mutant missorts to other cellular destinations. The fate of the mutant virus after leaving the endosome remains unknown. The observation that the GV mutant virus reaches the endosome but fails to bind to  $\gamma$ -secretase or insert into the membrane suggests that the GxxxG motif is important to target L2 to  $\gamma$ -secretase. This failure impairs proper Golgi targeting during infection. Cells infected with WT virus and treated with  $\gamma$ -secretase inhibitor XXI display a similar phenotype (Zhang et al., 2014).

#### **$\gamma$ -Secretase-dependent membrane insertion of L2 is required for retromer recruitment**

What is the functional importance of  $\gamma$ -secretase-mediated L2 membrane insertion during HPV infection? During successful infection, conserved sites in the C terminus of the L2 protein bind to retromer, a trafficking factor that sorts the incoming HPV virion to the retrograde pathway. Experiments with purified proteins demonstrated that binding between retromer and L2 is direct (Popa et al., 2015). The lack of Golgi targeting in cells treated with the  $\gamma$ -secretase inhibitor XXI (Zhang et al., 2014) led us to hypothesize that  $\gamma$ -secretase-dependent L2 membrane insertion might recruit retromer to the L2 protein. To test this, HeLa cells were infected with WT HPV16.L2F or GV HPV16.L2F in the presence or absence of XXI and after 8 h processed for PLA with antibodies recognizing FLAG and the retromer subunit, vacuolar protein sorting-associated protein 35 (VPS35), to detect recruitment of retromer to L2. In agreement with our previous reports (Lipovsky et al., 2013; Popa et al., 2015), bright PLA signals were observed in cells infected with WT HPV16.L2F (Fig. 6 A), showing that WT L2 recruits retromer. The PLA signal was markedly lower in infected cells treated with XXI (Fig. 6 A; quantified in Fig. 6 B), demonstrating that  $\gamma$ -secretase inhibition impaired L2 from recruiting retromer. Because the retromer is localized to the cytoplasm, these results suggest that exposure of L2 to the cytosol after membrane insertion is required for retromer recruitment.

We also tested retromer recruitment in cells infected with the GV mutant or treated with BafA1. Fig. 6 A shows that in cells infected with the GV HPV16.L2F mutant virus (in the absence of XXI) or in BafA1-treated cells infected with WT HPV16.L2F, PLA signals corresponding to the L2-retromer recruitment decreased significantly compared with signals in WT HPV16.L2F-infected

control cells (Fig. 6 A; quantified in Fig. 6 B). Because the mutant L2 protein cannot insert into the membrane (Fig. 5 C) during infection and BafA1 treatment blocked membrane insertion of WT L2 (Fig. 3 B), these results further support the notion that L2 insertion into the endosome membrane is required for recruitment of retromer to L2 and entry into the retrograde transport pathway.

## **Discussion**

This paper establishes a key missing link during HPV entry and reveals a novel nonproteolytic activity of  $\gamma$ -secretase.  $\gamma$ -Secretase plays an essential role during HPV infection by regulating the transport of the L2-viral genome complex from the endosome to the TGN (Zhang et al., 2014). In parallel, retromer, which normally delivers cellular TM cargos from the endosome to the TGN (Gallon and Cullen, 2015), directly binds the C terminus of L2 and targets the L2-viral genome complex from the endosome to the TGN (Lipovsky et al., 2013; Popa et al., 2015). Here we demonstrated that when HPV reaches the endosome,  $\gamma$ -secretase executes a novel chaperone function by binding to and promoting the low pH-dependent membrane insertion of L2 (Fig. 6 C). The L2 protein thus has the unusual property of converting into a membrane-inserted form during infection. Upon membrane insertion and protrusion into the cytoplasm, L2 recruits retromer, which in turn targets the L2-viral genome complex to the TGN/Golgi en route for successful infection. Although membrane-inserted L2 can also be cleaved by  $\gamma$ -secretase, this cleavage reaction appears to be dispensable during HPV infection. Similarly, the ability of a protease-deficient,  $\gamma$ -secretase mutant to support infection indicates that cleavage of cellular  $\gamma$ -secretase substrates is also dispensable for infection.

Membrane insertion requires not only  $\gamma$ -secretase but also furin activity and low pH, and the furin-cleaved form of L2 is preferentially inserted to the membrane. We envision that furin-cleaved L2 is recruited to the luminal side of the endosome membrane by associating with  $\gamma$ -secretase (Fig. 6 C). L2 then experiences a low pH-induced structural alteration that allows its C-terminal, low pH-dependent membrane-destabilizing domain (Kämper et al., 2006) to initiate membrane penetration. L2 protrudes through the endosome membrane until the TM domain near the N terminus of L2 arrives in the membrane bilayer. When this occurs, L2 is in a type I TM topology with its N terminus anchored in the capsid in the endosomal lumen and most of L2 including the retromer binding site protruding into the cytosol. The model that most of L2 is exposed in the cytoplasm is consistent with antibody staining and protease sensitivity experiments, as well as with the ability of the cytoplasmic protein SNX17 to bind to the middle of the L2 protein (Bergant Marušič et al., 2012; DiGiuseppe et al., 2015). Our results further revealed that conditions that disrupted  $\gamma$ -secretase-mediated membrane insertion of the L2 protein (i.e., inhibition of  $\gamma$ -secretase, BafA1 treatment, and mutation of the TM GxxxG sequence) all blocked retromer recruitment, explaining why HPV cannot reach the TGN/Golgi and infection does not proceed under these conditions. It is possible that  $\gamma$ -secretase binds directly to the L2 TM domain to facilitate membrane insertion, but further experiments are required to test this possibility.

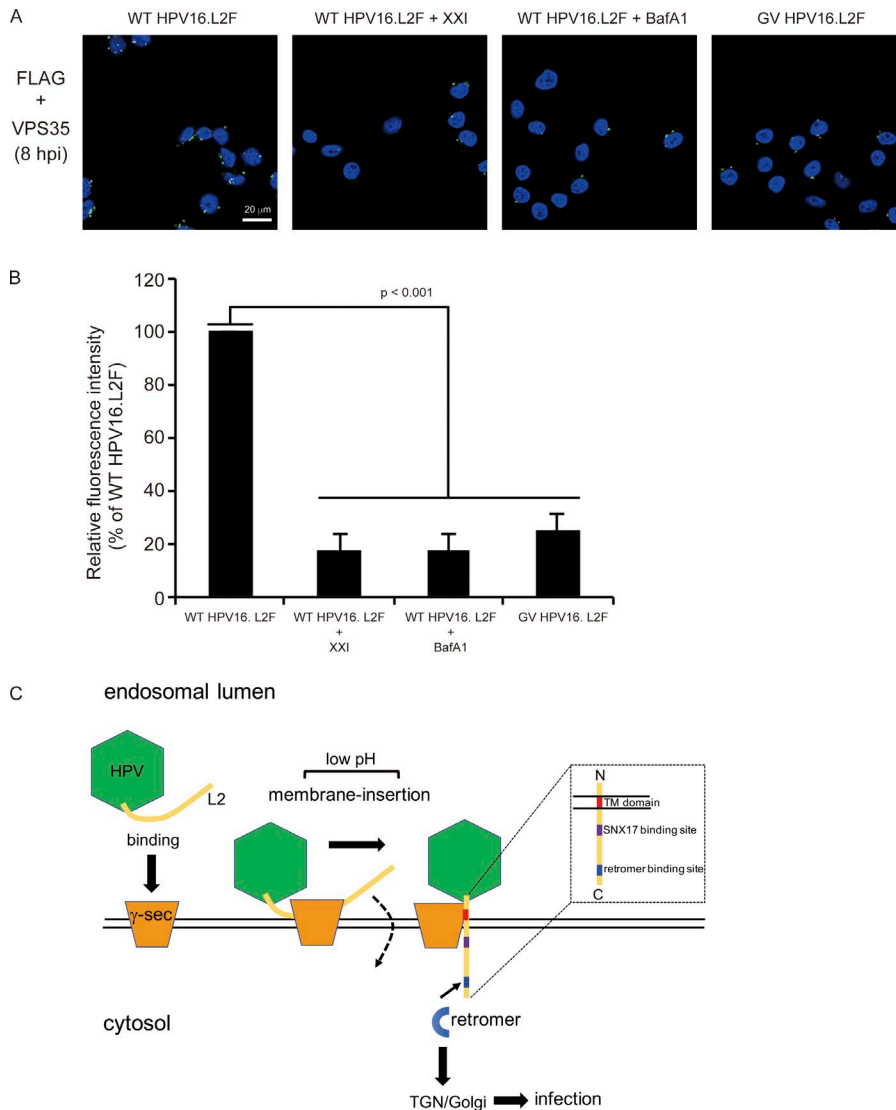


**Figure 6.  $\gamma$ -Secretase-dependent membrane insertion of L2 is required for retromer recruitment.** (A) HeLa cells were infected with WT HPV16.L2F in the absence or presence of 1  $\mu$ M XXI or 30 nM BafA1 or infected with GV HPV16.L2F in the absence of inhibitor. Cells were fixed at 8 hpi and subjected to the PLA assay using antibodies recognizing FLAG and VPS35 as in Fig. 5 E. (B) The PLA fluorescence intensities in A were quantified and shown as in Fig. 5 F, except that they were normalized to WT HPV16.L2F-infected cells at 8 hpi. The average VPS35/L2-3xFLAG intensity represents the means  $\pm$  standard deviations of data from at least three independent experiments. Student's two-tailed *t* test was used to assess statistical significance. (C) Model depicting how  $\gamma$ -secretase acts as a chaperone on the L2 capsid protein of HPV to promote infection. In the endosome,  $\gamma$ -secretase binds to L2 and in concert with the low pH promotes membrane insertion of L2. The L2 C terminus penetrates the endosome membrane, and most of L2 passes through the membrane until the TM domain at the L2 N terminus arrives in the membrane bilayer. When this occurs, L2 is in a type I TM topology. The cytosol-exposed retromer binding site in the L2 C terminus recruits the retromer, targeting the viral particle to the TGN/Golgi en route for successful infection. The inset indicates the TM domain, as well as the SNX17 and retromer binding sites, in L2.

Inhibition of retromer action by knockdown of retromer subunits or by mutations in the retromer binding sites in the L2 protein causes incoming viral components to accumulate in the endosome (Popa et al., 2015). In contrast, inhibition of  $\gamma$ -secretase impairs transport of the L2-viral genome complex to the TGN without causing endosomal accumulation. This implies that interfering with retromer-L2 association before membrane insertion causes viral components to be incorrectly sorted out of the endosome, whereas interfering after L2 protrusion into the cytoplasm results in endosome accumulation. Although some L1 is released from the incoming capsid during these endosomal events, it has recently been shown that some L1 travels with L2 and viral DNA to the nucleus (DiGiuseppe et al., 2017).

In sum, our results demonstrate that  $\gamma$ -secretase acts as a chaperone to promote membrane insertion of L2 during HPV entry. The identification of a novel chaperone activity associated with  $\gamma$ -secretase expands the postulated nonproteolytic functions of this enzyme (Otto et al., 2016) and raises the possibility that this activity affects cellular proteins. Beyond HPV-associated diseases, our discovery of the chaperone action of  $\gamma$ -secretase on L2 may have broader implications for cellular processes

that depend on this activity and for human diseases in which  $\gamma$ -secretase plays a pivotal role, such as Alzheimer's disease and several types of human cancers (Takebe et al., 2014; Selkoe and Hardy, 2016). The role of abnormal  $\gamma$ -secretase activity in these diseases has been ascribed to abnormal or absent cleavage of  $\gamma$ -secretase substrates. However, our findings raise the possibility that disease pathogenesis may in some cases instead reflect abnormal  $\gamma$ -secretase chaperone function.

## Materials and methods

### Antibodies and inhibitors

Antibodies and inhibitors used in this study are listed in Table 1.

### DNA constructs

p16sheLL and p5sheLL are generous gifts from Dr. John Schiller (National Cancer Institute, Rockville, MD; plasmids 37320 and 46953; Addgene). p16sheLL.L2F used to produce the WT HPV16.L2F PsV consisting of WT HPV16 L1 and FLAG-tagged L2 was previously described (Zhang et al., 2014). p5sheLL.L2F used to produce the HPV5.L2F PsV that consists of WT HPV5 L1 and

Table 1. List of antibodies and inhibitors used in this study

Antibodies			
Antigen	Species	Source	Application
FLAG M2	Mouse mono	F3165; Sigma	WB, IP, PLA
FLAG	Rabbit mono	F7425; Sigma	WB
NICA	Mouse mono	MAB53781; R&D Systems	WB
PS1 (CTF)	Rabbit mono	5643; CST	WB
PEN2	Mouse mono	5451; CST	WB
HSP27	Rabbit poly	SPA-903; Enzo	WB
GFP	Mouse mono	66002-1-Ig; Proteintech	WB
EEA1	Rabbit mono	C45B10; CST	PLA
TGN46	Rabbit poly	ab50595; Abcam	PLA
VPS35	Mouse mono	57632; Abcam	PLA
FLAG	Rabbit mono	2368; CST	PLA
Inhibitors			
Compound	Solvent	Source	Concentration
XXI	DMSO	565790; Millipore	0.1–3 $\mu$ M
dRVKR	DMSO	344930; Millipore	1 $\mu$ M
BafA1	DMSO	508409; Millipore	30 nM

IP, immunoprecipitation; WB, Western blot.

FLAG-tagged L2 was constructed from p5shell by inserting the 3xFLAG tag sequence in frame at the C terminus of the HPV5 L2 sequence. To construct p5sheLL.L2F, the following primers were used: 5'-CCCCGTCTTCGAAGAGGAGGTC-3', 5'-TCATGGTCTTTGTAGTACCAGAACCACCACCAGAACCACCGAGGTACTTGCCTTCCTC-3', 5'-GTCATCCTTGTAGTCGATGTCATGATCTTTATAATCACCGTCATGGTCTTTGTAGTACC-3', and 5'-ATATGCTAGCTCCTTGTAGTGCATCCTTGTAGTGCATGTC-3'.

Two glycine residues at L2 positions 57 and 61 were mutated to valine in p16sheLL.L2F to construct p16sheLL.L2FGV. The recombinant  $\gamma$ -secretase expression vector pMLink-Pen-2 + NCT + Aph-1 + PS1 (in which PEN2 is FLAG-tagged) was a generous gift from Dr. Yigong Shi (Tsinghua University, Beijing, China). To generate a DNA construct expressing an L2 fragment containing the TM domain fused to GFP with a C-terminal FLAG tagged (L2 (13–79)-GFP/FLAG), the following primers were used: 5'-ATATCTCGAGATGGCCAGCGCCACCCAGCTGTA-3', 5'-TCACTGGAGCAGGTGCTGGCCTGGTGGCCAGGGGATGTA-3', 5'-GCCAGCACC TGCTCCAGTGAGCAAGGGCGAGGAGCTGTTC-3', and 5'-ATATGGATCCTTACTTGTACAGCTCGTCCATGC-3'. Specifically, the cDNA sequence corresponding to this segment of L2 was amplified from p16shell and fused to a PCR-amplified EGFP sequence via an alanine–proline linker sequence (APAP) using an overlapping PCR method. The resulting PCR product was inserted into pcDNA3.1(-) in frame with the FLAG tag sequence. To insert the GV double mutant into L2 (13–79)-GFP/FLAG, p16sheLL.L2FGV was used as a template for PCR. To generate a DNA construct expressing WT PS1 constructs, the following primers were used: 5'-ATATCTCGAGATGACAGAGTTACCTGCACCG-3' and 5'-ATATGGATCCTAGATATAAACTGGTGAAAGGCCAACTGATCCATAAA

AGGCTGTACAAG-3'. Specifically, the WT cDNA sequence was amplified by PCR using pMLink-Pen-2 + NCT + Aph-1 + PS1 as a template, and the indicated mutations were introduced using an overlapping PCR method. The resulting PCR product was inserted into pcDNA3.1(-). To introduce L166P or F237I mutation on the WT PS1 cDNA, the following primers were used: for L166P, 5'-TATAGGGAGACCCAAGCTGGCTAGC-3', 5'-TAAGGTCATCCATGCCTGGCCATATATCATCTCTATTGTTG-3', 5'-GCCAGGCATGGA TGACCTTA-3', and 5'-TAAGCTTGGTACCGAGCTCGGATCC-3'; for F237I, 5'-TATAGGGAGACCCAAGCTGGCTAGC-3', 5'-ATCAAGTACCTCCCTGAATG-3', 5'-CATTCAGGGAGGTACTTGTATgAtCAC CAGGGCCATGAGGGCACTAA-3', and 5'-TAAGCTTGGTACCGA GCTCGGATCC-3'. We note that because cytomegalovirus immediate early promoter-driven L166P PS1 expression was poor compared with WT and the other mutant constructs, the L166P PS1 fragment derived from the corresponding pcDNA3.1(-) was subcloned into the CAG promoter-driven expression vector pCAG GS (Niwa et al., 1991).

### Cell culture

HeLa, HaCaT, and HEK 293T cells were obtained from American Type Culture Collection, and 293TT cells were obtained from Dr. Christopher Buck (National Cancer Institute, Rockville, MD). All cell lines were cultured in DMEM (Thermo Fisher Scientific) containing 10% fetal bovine serum (Corning), 10 U/ml penicillin (Thermo Fisher Scientific), and 10  $\mu$ g/ml streptomycin (Thermo Fisher Scientific). HeLa-Sen2 cells (Goodwin et al., 2000) were used for PLA assays.

### HPV PsV production

HPV PsVs containing reporter gene plasmids were produced by cotransfection of p16sheLL.L2F, p16sheLL.L2FGV, or p5sheLL.L2F and the indicated reporter gene plasmid into 293TT cells with polyethylenimine HCl MAX, Linear, molecular weight of 40,000 (Polysciences Inc.), and were isolated using an OptiPrep density gradient centrifugation as previously described (Buck et al., 2004, 2005). In brief, cells collected after transfection were treated with lysis buffer (0.5% Triton X-100, 10 mM MgCl<sub>2</sub>, 5 mM CaCl<sub>2</sub>, and 0.5 U/ml RNase A) and purified by centrifugation on an OptiPrep step gradient (27, 33, and 39%) at 300,000 g in an SW55 Ti rotor for 3.5 h. The infectious titer of WT PsV was determined by flow cytometry for fluorescent reporter protein expression in unmodified HeLa cells 48 h after infection. For some experiments, the number of viral genome equivalents in PsV preparations was determined by quantitative PCR (Zhang et al., 2014). To isolate viral reporter genome, purified WT and mutant HPV16 PsVs were pretreated with DNase I (Qiagen) to remove any free DNA associated with capsids. After inactivating the DNase I at 75°C for 30 min, the capsids were digested with proteinase K using DNeasy Blood and Tissue kits (Qiagen) to isolate genome reporter plasmids. The copy number of encapsidated reporter plasmids in WT and mutant PsV stocks was determined by quantitative PCR using primers for the reporter gene in comparison with a standard curve. Equivalent numbers of genomes in WT and mutant stocks were used in each experiment, with the MOI of mutants expressed as the MOI of WT containing the same number of packaged reporter plasmids.

We estimate that ~10–30 plasmids per cell represent a MOI of ~1 for WT PsV.

#### Affinity purification of HPV16.L2F from PsV-infected cells

Three 15-cm plates of HeLa cells at  $1.6 \times 10^7$  cells per plate were uninfected or infected with WT HPV16.L2F at MOI = 100 for 16 h, harvested, and lysed in 3 ml of a buffer containing 50 mM Hepes (pH 7.5), 150 mM NaCl (HN buffer), 1% Triton X-100, and 1 mM PMSF. After centrifugation at 16,100 g, the resulting supernatant fraction was incubated with FLAG M2 antibody (0.3  $\mu$ g/ml) at 4°C for 2 h, and the immune complex was captured with protein G-coated magnetic beads (Thermo Fisher Scientific). Lysate derived from uninfected cells was mixed with OptiPrep-isolated HPV16.L2F before incubation with FLAG M2 antibody and served as a background control that reveals postlysis binding proteins. The bound proteins were eluted with 0.1 mg/ml 3xFLAG peptide (Sigma) followed by precipitation with TCA. The TCA-precipitated materials were subjected to SDS-PAGE or mass spectrometry analysis (Taplin Mass Spectrometry Core Facility, Harvard Medical School).

#### Detection of immunoblotting signals

To detect chemiluminescence signals derived from HRP and ECL, membranes were detected using X-ray film. Membrane was exposed to X-ray film.

#### Detection of $\gamma$ -secretase-mediated L2 cleavage

HeLa cells were plated at  $5 \times 10^5$  cells per well in a six-well plate, incubated for 24 h, and infected with HPV16.L2F or HPV5.L2F at MOI = 100. At 16 hpi, cells were harvested and lysed in 70  $\mu$ l of HN buffer containing 1% Triton X-100 and 1 mM PMSF and centrifuged at 16,100 g for 10 min. The resulting S fraction was mixed with 30  $\mu$ l of 4 $\times$  SDS sample buffer and boiled at 95°C for 10 min. An aliquot of the sample (30  $\mu$ l) was subjected to SDS-PAGE, followed by semidry transfer onto a nitrocellulose membrane. The membrane was incubated in a buffer composed of 50 mM Tris (pH 7.4), 138 mM NaCl, 2.7 mM KCl, 0.2% tween-20, and 3% milk TBS-T containing 0.3  $\mu$ g/ml FLAG M2 antibody at 4°C for 16 h, washed extensively with TBS-T, and further incubated in milk TBS-T containing 2,000-fold diluted HRP-conjugated anti-mouse antibody (A4416; Sigma) at 25°C for 30 min. After the membrane was extensively washed with TBS-T to remove unbound secondary antibody, HRP on the membrane was reacted with Millipore Immobilon Western Chemiluminescent HRP substrates (EMD Millipore), and the resulting membrane was exposed to X-ray film.

#### Immunoprecipitation

HeLa cells were plated at  $1.2 \times 10^6$  cells per well in a 6-cm plate, incubated for 24 h, and infected with either HPV16.L2F or HPV5.L2F at MOI = 100. At the indicated time, cells were harvested and lysed in 165  $\mu$ l of HN buffer containing 1% wt/vol Decyl Maltose Neopentyl Glycol (Anatrace) and 1 mM PMSF and centrifuged at 16,100 g for 10 min. 150  $\mu$ l of the resulting supernatant was incubated with FLAG M2 antibody (0.3  $\mu$ g/ml) at 4°C for 2 h, and the immune complex was captured with protein G-coated magnetic beads. Bound proteins were eluted with 20  $\mu$ l of 2 $\times$  SDS sample

buffer and slowly denatured by incubating at 37°C for 30 min, followed by SDS-PAGE and immunoblotting using rabbit FLAG antibody and PS1 antibody.

#### Preparation of recombinant proteins

To isolate recombinant  $\gamma$ -secretase, 30–50% confluent HEK 293T cells were transfected with pMLink-Pen-2 + NCT + Aph-1 + PS1 (12.5  $\mu$ g per 15-cm plate) by using polyethylenimine, incubated for 48 h, harvested, and lysed in HN buffer containing 0.5% wt/vol digitonin (EMD Millipore) and 1 mM PMSF (1 ml/15 cm plate) at 4°C for 20 min. Following centrifugation at 16,100 g for 10 min, the resulting supernatant was incubated with anti-FLAG M2 antibody-conjugated agarose beads at 4°C for 2 h. The beads were recovered by centrifugation and washed with HN buffer containing 0.2% wt/vol CHAPSO (Anatrace). The  $\gamma$ -secretase complex was eluted with 0.1 mg/ml FLAG peptide in HN buffer containing 0.2% CHAPSO. To isolate L2 (13–79)-GFP/FLAG, 50–70% confluent HEK 293T cells were transfected with the appropriate DNA construct (5  $\mu$ g per 10-cm plate), incubated for 24 h, and subjected to the same procedure as for recombinant  $\gamma$ -secretase.

#### Coimmunoprecipitation between $\gamma$ -secretase and L2

Purified L2 (13–79)-GFP/FLAG (200 nM) mixed with or without purified  $\gamma$ -secretase (1  $\mu$ M) in 50  $\mu$ l of HN buffer containing 0.2% CHAPSO and 1 mM dithiobis succinimidyl propionate was incubated at 4°C for 16 h. Cross-linking was quenched with 1 mM Tris for 15 min at room temperature. The complex was captured by adding PS1 antibody to samples at 4°C for 1 h, followed by addition of protein G-coated magnetic beads for 1 h at 4°C. Following bead incubation, 30  $\mu$ l was collected from each sample to represent 50% of the unbound material. Beads were then washed three times in 200  $\mu$ l of HN buffer containing 0.2% CHAPSO, treated with 5 $\times$  SDS-sample buffer, denatured at 37°C for 30 min, and analyzed by SDS-PAGE and immunoblotting using M2-FLAG and anti-GFP antibodies.

#### In vitro L2 cleavage assay

Recombinant  $\gamma$ -secretase (1  $\mu$ M) and L2 (13–79)-GFP/FLAG (100 nM) were mixed in 20  $\mu$ l of HN buffer containing 0.2% CHAPSO wt/vol, 1 mM MgCl<sub>2</sub>, 1 mM CaCl<sub>2</sub>, and 1 mM DTT and incubated at 37°C for 16 h. Where indicated, DMSO (final concentration, 0.2% vol/vol) or XXI (final concentration, 10  $\mu$ M in 0.2% DMSO) was added to the reaction. After incubation, the samples were mixed with 8  $\mu$ l of 4 $\times$  SDS sample buffer, slowly denatured by incubating at 37°C for 30 min, and analyzed by SDS-PAGE and immunoblotting using anti-GFP antibody.

#### Infection experiments

HeLa cells were plated in a 24-well plate at a density of  $\sim 1.2 \times 10^5$  cells per well, incubated for 24 h, and infected with HPV16.L2F packaging a reporter gene plasmid encoding hcRed or a secreted gaussia luciferase. DMSO or inhibitors were added at the indicated time point. At 36 hpi, a portion of the culture supernatant (10  $\mu$ l each) was used to measure luciferase activity using the BioLux Gaussia Luciferase Assay kit (NEB) per the manufacturer's instructions. Alternatively, hcRed-expressing cells were analyzed by flow cytometry.

### siRNA transfection

The target sequences of the siRNAs used in this study are as follows: PS1 #1 siRNA: 5'-UCAAGUACCUCCUGAAUG-3'; PS1 #2 siRNA: 5'-CCAAUUAGCAUCCAUCAA-3'; PEN2 #1 siRNA: 5'-CCAAUGAGGAGAAAUUGAA-3'; PEN2 #2 siRNA: 5'-UCACCAUCUCCAGAUCUA-3'.

Allstar negative control siRNA (Qiagen) was used as a Scr control siRNA. HeLa or HaCaT cells were reverse-transfected with 30 nM siRNA using Lipofectamine RNAi MAX (Thermo Fisher Scientific) according to the manufacturer's instructions and incubated for 48 h before HPV PsV infection.

### Alkali extraction

HeLa cells were plated at  $3 \times 10^6$  cells in a 10-cm plate, incubated for 24 h, and infected with HPV16.L2F at MOI = 50. At the indicated time points, cells were harvested, resuspended in 1 ml of HN buffer, and homogenized by passing 12 times through a 10- $\mu$ m clearance ball bearing homogenizer (Isobiotec). The resulting cell homogenate was centrifuged at 16,100 g for 10 min to separate the cytosol and membrane fractions from the nuclear and mitochondrial fractions. The resulting supernatant was further centrifuged at 50,000 rpm in a TLA 100.3 rotor (Beckman) at 4°C for 30 min to separate the membrane fraction from the cytosol fraction. The resulting pellet containing the membrane fraction was gently washed with 180  $\mu$ l of HN buffer and centrifuged at 50,000 rpm in a TLA 100.3 rotor at 4°C for 10 min. The rinsed pellet was resuspended in 25  $\mu$ l of a buffer containing 10 mM Tris-HCl (pH 7.5), 150 mM NaCl, 2 mM MgCl<sub>2</sub>, 5 mM DTT, and 50 units Benzonase and incubated at 37°C for 30 min. The Benzonase-treated membrane fraction was mixed with 225  $\mu$ l of a buffer containing 0.1 M Na<sub>2</sub>CO<sub>3</sub> and 2–3 M urea without or with 1% Triton X-100, incubated on ice for 30 min, and centrifuged at 50,000 rpm in a TLA 100.3 rotor at 4°C for 30 min. After rinsing the resulting P fraction with 180  $\mu$ l of HN buffer as mentioned above, both S and P fractions were analyzed by immunoblotting with the indicated antibodies. For HaCaT cells, HPV16.L2F-infected cells were processed as above, except that 4 M urea was used.

### PLA

$5 \times 10^4$  HeLa-sen2 cells were seeded onto glass coverslips in a 24-well plate. After overnight incubation, the cells were infected with WT HPV16.L2F PsV or GV HPV16.L2F (corresponding to WT infectious MOI of 50). In some experiments, cells were treated with 1  $\mu$ M XXI. After 8 or 16 h, cells were fixed with 4% PFA, permeabilized with 1% saponin for 1 h at room temperature, and incubated with a mouse anti-FLAG antibody (no. F3165, 1:500 dilution; Sigma) and a 1:500 dilution of an anti-EEA1, anti-TGN46, or anti-VPS35 antibody at 4°C overnight. PLA was performed with the Duolink reagents from Olink Biosciences as previously described (Popa et al., 2015). In brief, samples were incubated with PLA probes in a humidified chamber for 1 h. After the probes were ligated for 30 min at 37°C, the ligation products were amplified and labeled with fluorescent oligonucleotides for 100 min at 37°C. Nuclei were stained by a 10-min incubation with 5  $\mu$ g/ml of DAPI. Images were captured with the Leica TCS SP5 microscope using HCX PL APO 63 $\times$  1.4 Oil objective and processed with the ImageJ software. At least

150 nuclei per sample were imaged. Statistical analysis was done with the Blobfinder software to determine the total fluorescence intensity per cell as previously described (Zhang et al., 2014; Lipovsky et al., 2015).

### CRISPR KO cells

pX330 and pX459 used for generating PS1 KO HeLa cells were gifts from Dr. Feng Zhang (Massachusetts Institute of Technology, Cambridge, MA; plasmids 42230 and 62988; Addgene). The following two oligonucleotides containing the +431 to +453 sequence from the transcriptional start site of the human PS1 (NM\_000021.3) were annealed and inserted into pX459: forward, 5'-CACCGTGGGGTCGTCCATTAGATAA-3'; reverse, 5'-AAACCTTATCTAATGGACGACCCAC-3'.

pX459 encoding the guide RNA or control pX330 was transfected into HeLa cells using Fugene HD (Promega), and at 24 h after transfection, the media were replaced with fresh media containing 0.6  $\mu$ g/ml puromycin. At 72 h after transfection, pX459 encoding the guide RNA or control pX330 was further transfected into HeLa cells using Fugene HD (Promega), and cells were further incubated in fresh media containing 0.6  $\mu$ g/ml puromycin. After most control cells had died, surviving cells transfected with the pX459 constructs were replated for single-colony isolation. When the single colonies were grown and became visible, they were isolated using cloning cylinders. The genome was also isolated from two independent cell lines and served as a template to amplify a region corresponding to the +39102 to +39524 sequence of *Homo sapiens* PS1 (RefSeqGene on chromosome 14, NG\_007386.2) using the following PCR primers: forward, 5'-AATGGAGCAAGCCAAGACC-3'; reverse, 5'-ACTCATAGTGACGGGTCTGTTG-3'. The amplified PCR product was subjected to agarose gel electrophoresis, and the corresponding band was excised from the gel and purified. The isolated DNA products were subjected to Sanger sequencing using the following primer: 5'-AATGGAGCAAGCCAAGACC-3' or 5'-ACTCATAGTGACGGGTCTGTTG-3'. Because a single band from the isolated PS1 CRISPR KO #1 genome was amplified and only one sharp peak was observed by Sanger analysis in which two C deletions were detected, we concluded that both alleles have the same mutation. In contrast, two different size bands were observed from the isolated PS1 CRISPR KO #2 genome. Each band was separately recovered from the agarose gel and analyzed by Sanger sequencing.

### PS1 add-back experiments

HeLa cells were plated at  $8 \times 10^4$  cells per well in a 24-well plate (for infection assay),  $3 \times 10^5$  cells per well in a 6-well plate (for cleavage assay), or  $10^6$  cells per well in a 6-cm plate (for alkali extraction). At 24 h after plating, 0.5, 2, and 4  $\mu$ g of the indicated DNA constructs were transfected to cells using Fugene HD (Promega). At 24 h after transfection, cells were infected with HPV16.L2F and processed for each assay as described above.

### Statistical analysis

Experimental values represent the means  $\pm$  standard deviations of data from at least three independent experiments. Student's two-tailed *t* test was used to assess statistical significance.

between two experimental data. P-values <0.05 were considered statistically significant.

### Online supplemental material

Fig. S1 shows that  $\gamma$ -secretase engages and cleaves L2 in the endosome after furin-mediated cleavage. Fig. S2 shows characterization of HPV16 infection in two distinct HeLa PS1 CRISPR KO cells (related to Fig. 4). Fig. S3 provides supporting data confirming that  $\gamma$ -secretase-dependent membrane insertion but not cleavage of L2 promotes HPV16 infection (related to Fig. 4).

### Acknowledgments

We thank Mac Crite for experimental assistance and Jan Zulkowski for assistance in preparing this manuscript.

W. Zhang was supported in part by the National Research Service Award (NRSA) F32 (AI114132). K. Goodner-Bingham was supported in part by an NRSA F31 (AI120486). This work was supported by the National Institutes of Health grants AI064296 and GM113722 to B. Tsai and AI102876 and CA016038 to D. DiMaio.

The authors declare no competing financial interests.

Author contributions: T. Inoue designed and performed experiments in Figs. 1–4 and 5, B–D. A. Dupzyk contributed to Figs. 1 J and 2 A. P. Zhang and W. Zhang performed PLA assays in Figs. 5 E and 6 A. K. Goodner-Bingham constructed the GV mutant and performed infection assays in Fig. 5 A. T. Inoue, D. DiMaio, and B. Tsai conceived the project, designed the experiments, and wrote the manuscript.

Submitted: 25 April 2018

Revised: 5 June 2018

Accepted: 25 June 2018

### References

Aydin, I., S. Weber, B. Snijder, P. Samperio Ventayol, A. Kühbacher, M. Becker, P.M. Day, J.T. Schiller, M. Kann, L. Pelkmans, et al. 2014. Large scale RNAi reveals the requirement of nuclear envelope breakdown for nuclear import of human papillomaviruses. *PLoS Pathog.* 10:e1004162. <https://doi.org/10.1371/journal.ppat.1004162>

Aydin, I., R. Villalonga-Planells, L. Greune, M.P. Bronnimann, C.M. Calton, M. Becker, K.Y. Lai, S.K. Campos, M.A. Schmidt, and M. Schelhaas. 2017. A central region in the minor capsid protein of papillomaviruses facilitates viral genome tethering and membrane penetration for mitotic nuclear entry. *PLoS Pathog.* 13:e1006308. <https://doi.org/10.1371/journal.ppat.1006308>

Beel, A.J., and C.R. Sanders. 2008. Substrate specificity of gamma-secretase and other intramembrane proteases. *Cell. Mol. Life Sci.* 65:1311–1334. <https://doi.org/10.1007/s00018-008-7462-2>

Bergant, M., and L. Banks. 2013. SNX17 facilitates infection with diverse papillomavirus types. *J. Virol.* 87:1270–1273. <https://doi.org/10.1128/JVI.01991-12>

Bergant Marušič, M., M.A. Ozbun, S.K. Campos, M.P. Myers, and L. Banks. 2012. Human papillomavirus L2 facilitates viral escape from late endosomes via sorting nexin 17. *Traffic.* 13:455–467. <https://doi.org/10.1111/j.1600-0854.2011.01320.x>

Bronnimann, M.P., J.A. Chapman, C.K. Park, and S.K. Campos. 2013. A transmembrane domain and GxxxG motifs within L2 are essential for papillomavirus infection. *J. Virol.* 87:464–473. <https://doi.org/10.1128/JVI.01539-12>

Buck, C.B., D.V. Pastrana, D.R. Lowy, and J.T. Schiller. 2004. Efficient intracellular assembly of papillomaviral vectors. *J. Virol.* 78:751–757. <https://doi.org/10.1128/JVI.78.2.751-757.2004>

Buck, C.B., D.V. Pastrana, D.R. Lowy, and J.T. Schiller. 2005. Generation of HPV pseudovirions using transfection and their use in neutralization assays. *Methods Mol. Med.* 119:445–462.

Buck, C.B., N. Cheng, C.D. Thompson, D.R. Lowy, A.C. Steven, J.T. Schiller, and B.L. Trus. 2008. Arrangement of L2 within the papillomavirus capsid. *J. Virol.* 82:5190–5197. <https://doi.org/10.1128/JVI.02726-07>

Calton, C.M., M.P. Bronnimann, A.R. Manson, S. Li, J.A. Chapman, M. Suarez-Berumen, T.R. Williamson, S.K. Molugu, R.A. Bernal, and S.K. Campos. 2017. Translocation of the papillomavirus L2/vDNA complex across the limiting membrane requires the onset of mitosis. *PLoS Pathog.* 13:e1006200. <https://doi.org/10.1371/journal.ppat.1006200>

Campos, S.K. 2017. Subcellular trafficking of the papillomavirus genome during initial infection: The remarkable abilities of minor capsid protein L2. *Viruses.* 9:370. <https://doi.org/10.3390/v9120370>

Cerqueira, C., Y. Liu, L. Kühling, W. Chai, W. Hafezi, T.H. van Kuppevelt, J.E. Kühn, T. Feitzl, and M. Schelhaas. 2013. Heparin increases the infectivity of Human Papillomavirus type 16 independent of cell surface proteoglycans and induces L1 epitope exposure. *Cell. Microbiol.* 15:1818–1836.

Cerqueira, C., P. Samperio Ventayol, C. Vogeley, and M. Schelhaas. 2015. Kallikrein-8 proteolytically processes human papillomaviruses in the extracellular space to facilitate entry into host cells. *J. Virol.* 89:7038–7052. <https://doi.org/10.1128/JVI.00234-15>

Day, P.M., R. Gambhira, R.B. Roden, D.R. Lowy, and J.T. Schiller. 2008. Mechanisms of human papillomavirus type 16 neutralization by L2 cross-neutralizing and L1 type-specific antibodies. *J. Virol.* 82:4638–4646. <https://doi.org/10.1128/JVI.00143-08>

Day, P.M., C.D. Thompson, R.M. Schowalter, D.R. Lowy, and J.T. Schiller. 2013. Identification of a role for the trans-Golgi network in human papillomavirus 16 pseudovirus infection. *J. Virol.* 87:3862–3870. <https://doi.org/10.1128/JVI.03222-12>

DiGiuseppe, S., T.R. Keiffer, M. Bienkowska-Haba, W. Luszczyk, L.G. Guion, M. Müller, and M. Sapp. 2015. Topography of the human papillomavirus minor capsid protein L2 during vesicular trafficking of infectious entry. *J. Virol.* 89:10442–10452. <https://doi.org/10.1128/JVI.01588-15>

DiGiuseppe, S., M. Bienkowska-Haba, L.G.M. Guion, T.R. Keiffer, and M. Sapp. 2017. Human papillomavirus major capsid protein L1 remains associated with the incoming viral genome throughout the entry process. *J. Virol.* 91:e00537-17. <https://doi.org/10.1128/JVI.00537-17>

Forman, D., C. de Martel, C.J. Lacey, I. Soerjomataram, J. Lortet-Tieulent, L. Bruni, J. Vignat, J. Ferlay, F. Bray, M. Plummer, and S. Franceschi. 2012. Global burden of human papillomavirus and related diseases. *Vaccine.* 30(Suppl. 5):F12–F23. <https://doi.org/10.1016/j.vaccine.2012.07.055>

Fujiki, Y., A.L. Hubbard, S. Fowler, and P.B. Lazarow. 1982. Isolation of intracellular membranes by means of sodium carbonate treatment: Application to endoplasmic reticulum. *J. Cell Biol.* 93:97–102. <https://doi.org/10.1083/jcb.93.1.97>

Gallon, M., and P.J. Cullen. 2015. Retromer and sorting nexins in endosomal sorting. *Biochem. Soc. Trans.* 43:33–47. <https://doi.org/10.1042/BST20140290>

Giroglou, T., L. Florin, F. Schäfer, R.E. Streeck, and M. Sapp. 2001. Human papillomavirus infection requires cell surface heparan sulfate. *J. Virol.* 75:1565–1570. <https://doi.org/10.1128/JVI.75.3.1565-1570.2001>

Goodwin, E.C., E. Yang, C.J. Lee, H.W. Lee, D. DiMaio, and E.S. Hwang. 2000. Rapid induction of senescence in human cervical carcinoma cells. *Proc. Natl. Acad. Sci. USA.* 97:10978–10983. <https://doi.org/10.1073/pnas.97.20.10978>

Hildesheim, A., R. Herrero, S. Wacholder, A.C. Rodriguez, D. Solomon, M.C. Bratti, J.T. Schiller, P. Gonzalez, G. Dubin, C. Porras, et al. Costa Rican HPV Vaccine Trial Group. 2007. Effect of human papillomavirus 16/18 L1 viruslike particle vaccine among young women with preexisting infection: a randomized trial. *JAMA.* 298:743–753. <https://doi.org/10.1001/jama.298.7.743>

Huang, H.S., C.B. Buck, and P.F. Lambert. 2010. Inhibition of gamma secretase blocks HPV infection. *Virology.* 407:391–396. <https://doi.org/10.1016/j.virol.2010.09.002>

Johnson, K.M., R.C. Kines, J.N. Roberts, D.R. Lowy, J.T. Schiller, and P.M. Day. 2009. Role of heparan sulfate in attachment to and infection of the murine female genital tract by human papillomavirus. *J. Virol.* 83:2067–2074. <https://doi.org/10.1128/JVI.02190-08>

Joyce, J.G., J.S. Tung, C.T. Przysiecki, J.C. Cook, E.D. Lehman, J.A. Sands, K.U. Jansen, and P.M. Keller. 1999. The L1 major capsid protein of human papillomavirus type 11 recombinant virus-like particles interacts with heparin and cell-surface glycosaminoglycans on human keratinocytes. *J. Biol. Chem.* 274:5810–5822. <https://doi.org/10.1074/jbc.274.9.5810>

- Kämper, N., P.M. Day, T. Nowak, H.C. Selinka, L. Florin, J. Bolscher, L. Hilbig, J.T. Schiller, and M. Sapp. 2006. A membrane-destabilizing peptide in capsid protein L2 is required for egress of papillomavirus genomes from endosomes. *J. Virol.* 80:759–768. <https://doi.org/10.1128/JVI.80.2.759-768.2006>
- Karanam, B., S. Peng, T. Li, C. Buck, P.M. Day, and R.B. Roden. 2010. Papillomavirus infection requires gamma secretase. *J. Virol.* 84:10661–10670. <https://doi.org/10.1128/JVI.01081-10>
- Kwak, K., R. Jiang, J.W. Wang, S. Jagu, R. Kirnbauer, and R.B. Roden. 2014. Impact of inhibitors and L2 antibodies upon the infectivity of diverse alpha and beta human papillomavirus types. *PLoS One.* 9:e97232. <https://doi.org/10.1371/journal.pone.0097232>
- Lee, L.Y., and S.M. Garland. 2017. Human papillomavirus vaccination: The population impact. *F1000 Res.* 6:866. <https://doi.org/10.12688/f1000research.10691.1>
- Li, Y., S.H. Lu, C.J. Tsai, C. Bohm, S. Qamar, R.B. Dodd, W. Meadows, A. Jeon, A. McLeod, F. Chen, et al. 2014. Structural interactions between inhibitor and substrate docking sites give insight into mechanisms of human PS1 complexes. *Structure.* 22:125–135. <https://doi.org/10.1016/j.str.2013.09.018>
- Lipovsky, A., A. Popa, G. Pimienta, M. Wyler, A. Bhan, L. Kuruvilla, M.A. Guie, A.C. Poffenberger, C.D. Nelson, W.J. Atwood, and D. DiMaio. 2013. Genome-wide siRNA screen identifies the retromer as a cellular entry factor for human papillomavirus. *Proc. Natl. Acad. Sci. USA.* 110:7452–7457. <https://doi.org/10.1073/pnas.1302164110>
- Lipovsky, A., W. Zhang, A. Iwasaki, and D. DiMaio. 2015. Application of the proximity-dependent assay and fluorescence imaging approaches to study viral entry pathways. *Methods Mol. Biol.* 1270:437–451. [https://doi.org/10.1007/978-1-4939-2309-0\\_30](https://doi.org/10.1007/978-1-4939-2309-0_30)
- Lu, P., X.C. Bai, D. Ma, T. Xie, C. Yan, L. Sun, G. Yang, Y. Zhao, R. Zhou, S.H.W. Scheres, and Y. Shi. 2014. Three-dimensional structure of human  $\gamma$ -secretase. *Nature.* 512:166–170. <https://doi.org/10.1038/nature13567>
- Mallon, R.G., D. Wojciechowicz, and V. Defendi. 1987. DNA-binding activity of papillomavirus proteins. *J. Virol.* 61:1655–1660.
- Niwa, H., K. Yamamura, and J. Miyazaki. 1991. Efficient selection for high-expression transfectants with a novel eukaryotic vector. *Gene.* 108:193–199. [https://doi.org/10.1016/0378-1119\(91\)90434-D](https://doi.org/10.1016/0378-1119(91)90434-D)
- Otto, G.P., D. Sharma, and R.S. Williams. 2016. Non-catalytic roles of presenilin throughout evolution. *J. Alzheimers Dis.* 52:1177–1187. <https://doi.org/10.3233/JAD-150940>
- Pim, D., J. Broniarczyk, M. Bergant, M.P. Playford, and L. Banks. 2015. A novel PDZ domain interaction mediates the binding between human papillomavirus 16 L2 and sorting nexin 27 and modulates virion trafficking. *J. Virol.* 89:10145–10155. <https://doi.org/10.1128/JVI.01499-15>
- Popa, A., W. Zhang, M.S. Harrison, K. Goodner, T. Kazakov, E.C. Goodwin, A. Lipovsky, C.G. Burd, and D. DiMaio. 2015. Direct binding of retromer to human papillomavirus type 16 minor capsid protein L2 mediates endosome exit during viral infection. *PLoS Pathog.* 11:e1004699. <https://doi.org/10.1371/journal.ppat.1004699>
- Pyeon, D., S.M. Pearce, S.M. Lank, P. Ahlquist, and P.F. Lambert. 2009. Establishment of human papillomavirus infection requires cell cycle progression. *PLoS Pathog.* 5:e1000318. <https://doi.org/10.1371/journal.ppat.1000318>
- Richards, R.M., D.R. Lowy, J.T. Schiller, and P.M. Day. 2006. Cleavage of the papillomavirus minor capsid protein, L2, at a furin consensus site is necessary for infection. *Proc. Natl. Acad. Sci. USA.* 103:1522–1527. <https://doi.org/10.1073/pnas.0508815103>
- Russ, W.P., and D.M. Engelman. 2000. The GxxxG motif: A framework for transmembrane helix-helix association. *J. Mol. Biol.* 296:911–919. <https://doi.org/10.1006/jmbi.1999.3489>
- Schelhaas, M., B. Shah, M. Holzer, P. Blattmann, L. Kühling, P.M. Day, J.T. Schiller, and A. Helenius. 2012. Entry of human papillomavirus type 16 by actin-dependent, clathrin- and lipid raft-independent endocytosis. *PLoS Pathog.* 8:e1002657. <https://doi.org/10.1371/journal.ppat.1002657>
- Selkoe, D.J., and J. Hardy. 2016. The amyloid hypothesis of Alzheimer's disease at 25 years. *EMBO Mol. Med.* 8:595–608. <https://doi.org/10.15252/emmm.201606210>
- Smith, J.L., S.K. Campos, A. Wandinger-Ness, and M.A. Ozbun. 2008. Caveolin-1-dependent infectious entry of human papillomavirus type 31 in human keratinocytes proceeds to the endosomal pathway for pH-dependent uncoating. *J. Virol.* 82:9505–9512. <https://doi.org/10.1128/JVI.01014-08>
- Sun, L., R. Zhou, G. Yang, and Y. Shi. 2017. Analysis of 138 pathogenic mutations in presenilin-1 on the in vitro production of A $\beta$ 42 and A $\beta$ 40 peptides by  $\gamma$ -secretase. *Proc. Natl. Acad. Sci. USA.* 114:E476–E485. <https://doi.org/10.1073/pnas.1618657114>
- Takasugi, N., T. Tomita, I. Hayashi, M. Tsuruoka, M. Niimura, Y. Takahashi, G. Thinakaran, and T. Iwatsubo. 2003. The role of presenilin cofactors in the gamma-secretase complex. *Nature.* 422:438–441. <https://doi.org/10.1038/nature01506>
- Takebe, N., D. Nguyen, and S.X. Yang. 2014. Targeting notch signaling pathway in cancer: Clinical development advances and challenges. *Pharmacol. Ther.* 141:140–149. <https://doi.org/10.1016/j.pharmthera.2013.09.005>
- Wang, J.W., and R.B. Roden. 2013. L2, the minor capsid protein of papillomavirus. *Virology.* 445:175–186. <https://doi.org/10.1016/j.virol.2013.04.017>
- Woodham, A.W., D.M. Da Silva, J.G. Skeate, A.B. Raff, M.R. Ambroso, H.E. Brand, J.M. Isas, R. Langen, and W.M. Kast. 2012. The S100A10 subunit of the annexin A2 heterotetramer facilitates L2-mediated human papillomavirus infection. *PLoS One.* 7:e43519. <https://doi.org/10.1371/journal.pone.0043519>
- Zhang, W., T. Kazakov, A. Popa, and D. DiMaio. 2014. Vesicular trafficking of incoming human papillomavirus 16 to the Golgi apparatus and endoplasmic reticulum requires  $\gamma$ -secretase activity. *MBio.* 5:e01777-14. <https://doi.org/10.1128/mBio.01777-14>